

A Comprehensive Review of the Pharmacological Potential of Green Synthesized Nanoparticles from *Calotropis procera*

Gauri Shankar Bhardwaj, Aditya Jain, Tanvi Jangid, Ram Niwas Jangir*

Department of Zoology, University of Rajasthan, Jaipur, Rajasthan, INDIA.

ABSTRACT

Calotropis procera is a versatile plant widely recognized for its applications in traditional medicine, fodder, fuel, timber, fibre production, and phytoremediation. In recent years, it has also gained attention in nanotechnology research as a green source for nanoparticle synthesis. Green-synthesized nanoparticles have emerged as a major focus due to their environmentally friendly, sustainable, and biocompatible nature. Among various biological sources, plants like *C. procera* are commonly employed for nanoparticle synthesis owing to their inherent safety, rich phytochemical profile, and ecological benefits. This review summarizes in-depth analysis of global research on *Calotropis procera*-based nanoparticles by examining literature from major scientific databases, including PubMed, Scopus, Web of Science, and Google Scholar, covering studies published up to 2025. This review provides a comprehensive overview of the botanical characteristics, key phytochemical constituents, and traditional uses of *Calotropis procera*. It also explores the different types of nanoparticles synthesized from *C. procera* and their major pharmacological activities, including antimicrobial, antidiabetic, anti-inflammatory, anti-cancerous, larvicidal, immunomodulatory, anti-hypertensive, anti-oxidant and hepatoprotective activity, as well as the toxicity profile of *C. procera*-derived green nanoparticles. In conclusion, nanoparticles synthesized from *Calotropis procera* hold significant promise as therapeutic agents due to their diverse pharmacological properties. Through this review, a strong platform is established for future research on *C. procera*-based nanoparticles for clinical and other applications.

Keywords: *Calotropis procera*, Green synthesized Nanoparticles, Pharmacological Properties, Phytochemical Composition, Toxicity.

Correspondence:

Ram Niwas Jangir

Department of Zoology, University of Rajasthan, Jaipur, Rajasthan, INDIA.
Email: ramanjangir@gmail.com

Received: 08-05-2025;

Revised: 24-07-2025;

Accepted: 12-09-2025.

INTRODUCTION

Medicinal plants are an essential part of daily life and are widely utilized for treating a variety of diseases and health conditions.^[1] Plant-mediated Nanoparticles (NPs) are increasingly favored over chemically synthesized alternatives due to their environmentally friendly nature and reduced ecological impact.^[2]

Calotropis procera (*C. procera*), a member of the Asclepiadaceae family, is known by various names worldwide, such as swallowwort, Sodom apple, dead sea apple, and milkweed. In India, it is commonly identified as orka in Oriya, madar in Hindi, alarka in Sanskrit, and akanda in Bengali. In Ayurvedic medicine, particularly in the formulation Arkelavana, it is referred to as Aak. Renowned for its potent medicinal properties, *C. procera* is highly valued in traditional medicine for its therapeutic potential.^[3] The genus name *Calotropis* originates from Greek,

signifying "beautiful," a reference to the plant's visually attractive flowers. The species name *procera*, on the other hand, is derived from Latin and is associated with the plant's distinctive waxy coating found on its leaves and stems.^[4] It thrives and sustains growth under harsh environmental conditions such as drought, high salinity, extreme temperatures, low humidity, and intense sunlight.^[5]

Over the past few decades, nanotechnology has experienced tremendous growth, not only in the diversity of its applications-including biomedical, healthcare, drug delivery, environmental protection, electronics, magnetism, space science, sensors, and energy storage and conversion-but also in the rising number of industrial R&D companies actively and effectively incorporating nanotechnology into their respective fields.^[6] Nanoparticles (NPs), owing to their nanoscale dimensions (1-100 nm), exhibit unique physicochemical and biological characteristics. Depending on their shape, size, and dispersion, NPs exhibit superior characteristics and enhanced functionality compared to their bulk material counterparts.^[7,8] Moreover, the increased surface area-to-volume ratio of nanoparticles is crucial and significantly enhances their efficiency in various



DOI: 10.5530/phrev.20250016

Copyright Information :

Copyright Author (s) 2025 Distributed under
Creative Commons CC-BY 4.0

Publishing Partner : Manuscript Technomedia, [www.mstechnomedia.com]

biological applications. The use of individual phytochemicals leads to the production of highly stable Nanoparticles (NPs). The quality of nanoparticles is affected by the hydroxyl functional groups present in these phytochemicals.^[9] To boost antioxidant performance, nanotechnology enhances the stability of bioactive molecules, improves their bioavailability, and ensures accurate delivery to specific biological targets.^[10]

Despite the increasing interest in plant-mediated green synthesis of nanoparticles, there is a lack of comprehensive reviews focusing specifically on *Calotropis procera*. Although several primary studies have reported the synthesis and pharmacological evaluation of nanoparticles derived from different parts of this plant, no single review article has consolidated these findings. Most existing literature either focuses on general green synthesis methods or on other medicinal plants, leaving a significant gap in understanding the full therapeutic potential and mechanistic insights of *C. procera*-based nanoparticles. Moreover, the integration of its ethnobotanical relevance, phytochemical richness, and toxicity profile in the context of nanoparticle synthesis remains underexplored.

This review is the first to comprehensively compile and critically evaluate the green synthesis of a wide range of nanoparticles-such as silver, gold, copper, and various metal oxides-using different parts of *Calotropis procera*. It highlights the unique correlation between the plant's diverse phytochemical profile and the pharmacological activities exhibited by these biosynthesized nanoparticles, including antidiabetic, larvicidal, antimicrobial, anticancer, antioxidant, hepatoprotective, immunomodulatory, antihypertensive, and anti-inflammatory effects. The review further strengthens its scientific value by incorporating a detailed toxicity profile, offering insights into both safety and efficacy. To enhance clarity and accessibility, all pharmacological activities have been concisely summarized in a tabular format. By integrating aspects of ethnopharmacology, nanobiotechnology, and therapeutic potential, this work provides a novel and holistic perspective on the biomedical relevance of *C. procera*-based nanoparticles.

BOTANICAL PROFILE

C. procera is a perennial, evergreen shrub or soft-wooded tree that can grow up to 2.5 m in height, with a maximum height of 6 m. The stem is typically unbranched and simple, with a woody base covered in fissured, corky bark. When any part of plant cut or broken, the plant releases white latex. Its root system consists of a taproot extending approximately 3 to 4 m deep and woody at base.^[11] The leaves are arranged in an opposite-decussate pattern, simple, subsessile and exstipulate. They have a slightly leathery texture and are covered with a fine layer of soft hairs, which may occasionally cause a stinging sensation.^[12]

TRADITIONAL USES

India is a prominent tropical country abundant in natural resources and traditional knowledge related to their use. *C. procera* is one such significant medicinal plant, highly valued for its rich ethnobotanical applications and substantial economic importance.^[13] Traditionally, some parts of the plant are known for their medicinal benefits to treat various ailments. The whole plant has been utilized for managing rheumatism, fever, indigestion, colds, eczema, diarrhea, boils and jaundice. The root has been employed in the treatment of eczema, leprosy, elephantiasis, asthma, cough, rheumatism and diarrhea, while the stem has been used for conditions such as leprosy, intestinal worms and leukoderma.^[14,15] The latex used in medications for treating *Tinea capitis* in children due to its antifungal properties, also has a historical record of more drastic applications inducing abortion in women.^[16] The flowers were thought to enhance digestion, alleviate mucus buildup, and boost appetite. The blooming tops were utilized for managing asthma. Moreover, the root bark was applied in the therapy of elephantiasis.^[12,17]

PHYTOCHEMICAL COMPOSITION

Phytochemical analysis of *C. procera* has identified the presence of numerous bioactive constituents in substantial quantities, including alkaloids, flavonoids, tannins, saponins, anthraquinones, sesquiterpenes, steroids, terpenes, and cardiac glycosides.^[18,19] The major cardioactive glycosides identified in *C. procera* include calactin, calotoxin, usharin, usharidine, and vouscharin. Among the plant parts, the latex exhibits the highest concentration of cardenolides, with uscharin and calotropagenin being the dominant compounds. In the leaves, calotropin and calotropagenin are primarily found, while the stem contains key cardenolides such as uscharidin, calotropin, proceroside, and calactin. The root bark primarily contains calotoxin and calactin, while the fruit pericarp is abundant in coroglaucigenin and uzarigenin. The seeds possess about 0.23-0.47% cardenolides, with coroglaucigenin or frugoside being the major constituents.^[12,20,21] Rutin (quercetin-3-rutinoside) is the major flavonoid found in *C. procera*, with its concentration differing among various parts of the plant. In addition to flavonoids, the plant is rich in a range of bioactive compounds including fatty acids, resins, proteolytic enzymes, amino acids, hydrocarbons, and essential minerals.^[22]

The flowers of *C. procera* are abundant in a wide range of bioactive compounds. These include flavonoids such as quercetin-3-rutinoside and sterols like β -sitosterol, β -sitost-4-en-3-one, stigmasterol, as well as α - and β -amyrins. In addition, they contain polysaccharides composed of sugars like D-arabinose, glucose, glucosamine, and L-rhamnose, along with significant cardenolides such as calactin, calotoxin, calotropagenin, and calotropin.^[23,24]

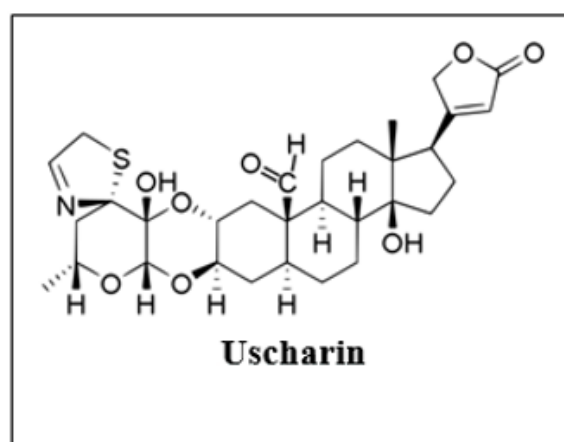
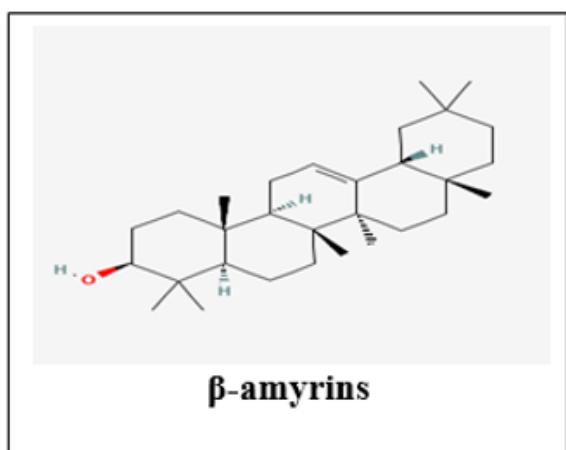
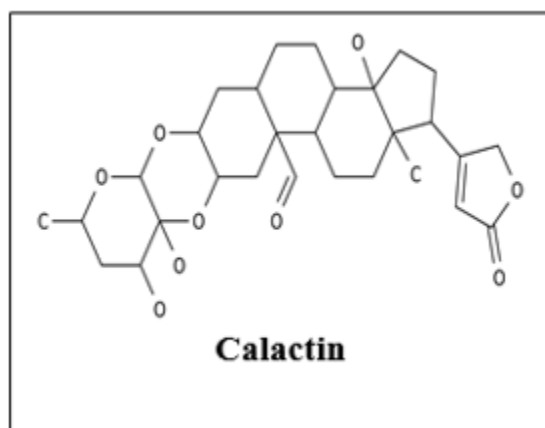
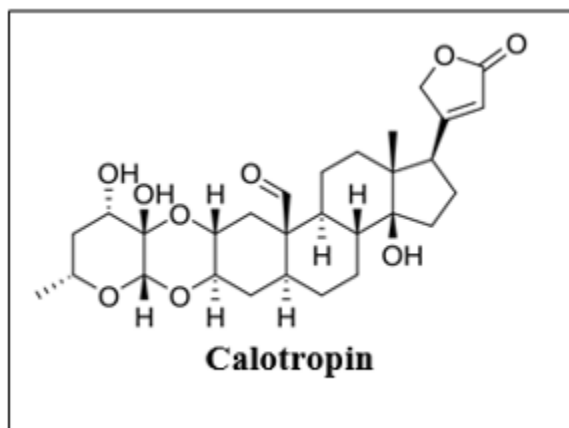
The roots of *C. procera* contain key phytochemicals such as cardenolides (calotoxin, *procera* genin), terpenes (calotropenol, calotropenyl acetate), and steroidal compounds like stigmasterol, β -sitosterol, and procesterol.^[25,26]

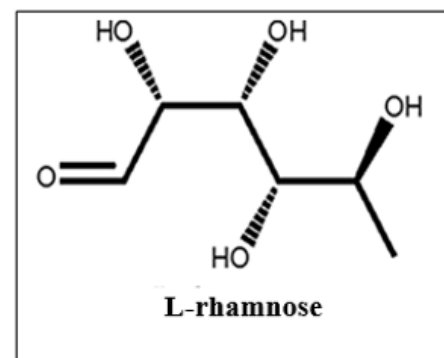
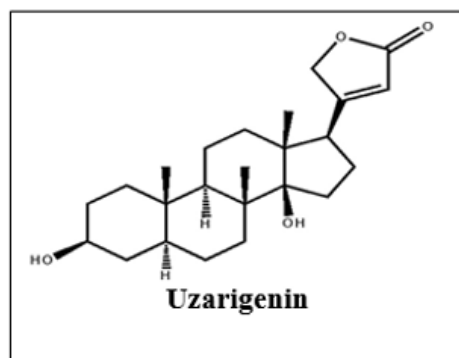
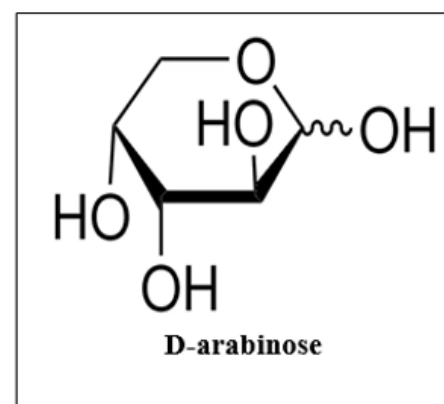
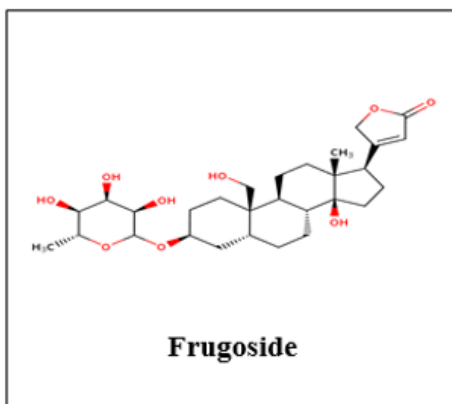
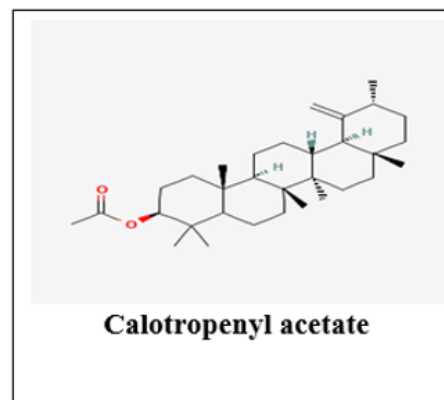
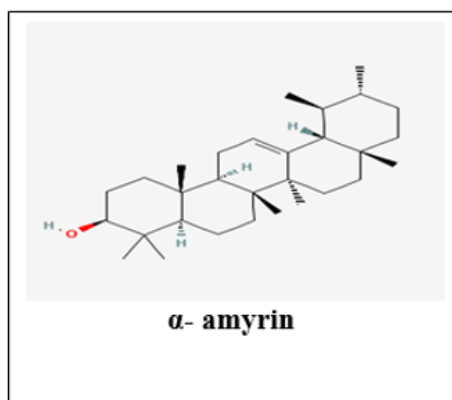
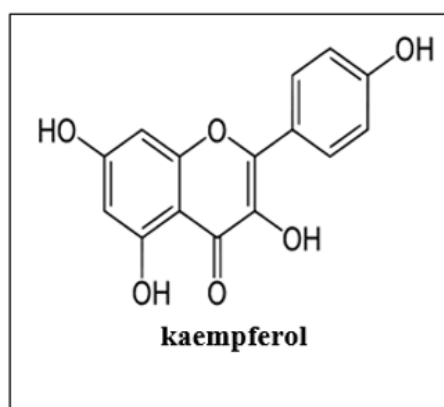
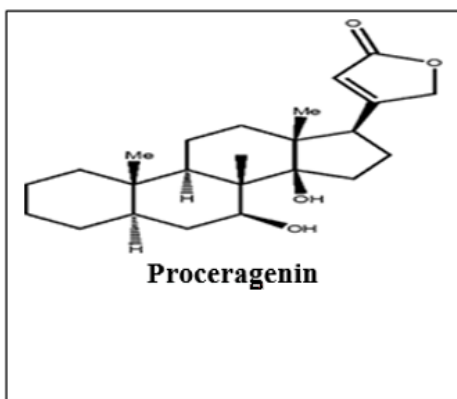
The leaves of *C. procera* are rich in important phytochemicals, including cardenolides such as calactin, calotoxin, calotropagenin, and calotropin. They also contain key flavonoids like kaempferol, isorhamnetin-3-O-rutinoside, and rutin, which contribute to antioxidant activity. Additionally, the leaves possess β -sitosterol and stigmasterol (steroidal compounds), ascorbic acid, and notable volatile constituents like R-limonene and tridecane.^[27-29]

The latex of *C. procera* contains several important bioactive compounds, notably cardenolides such as calactin, calotoxin, uscharin, and procegenins A and B. Key steroids include β -sitosterol and ursolic acid derivatives. It is also rich in proteins and enzymes like cysteine peptidases (CpCP-1, CpCP-2, CpCP-3) and procerain B. Among lignans, notable compounds include (+) Pinoresinol 4-O-[6-O-protocatechuoyl]- β -D glucopyranoside and its glycosylated derivatives.^[30,31]

Structure of various phytochemicals have been illustrated in Figure 1.

Major Phytochemical Structures of *Calotropis procera*





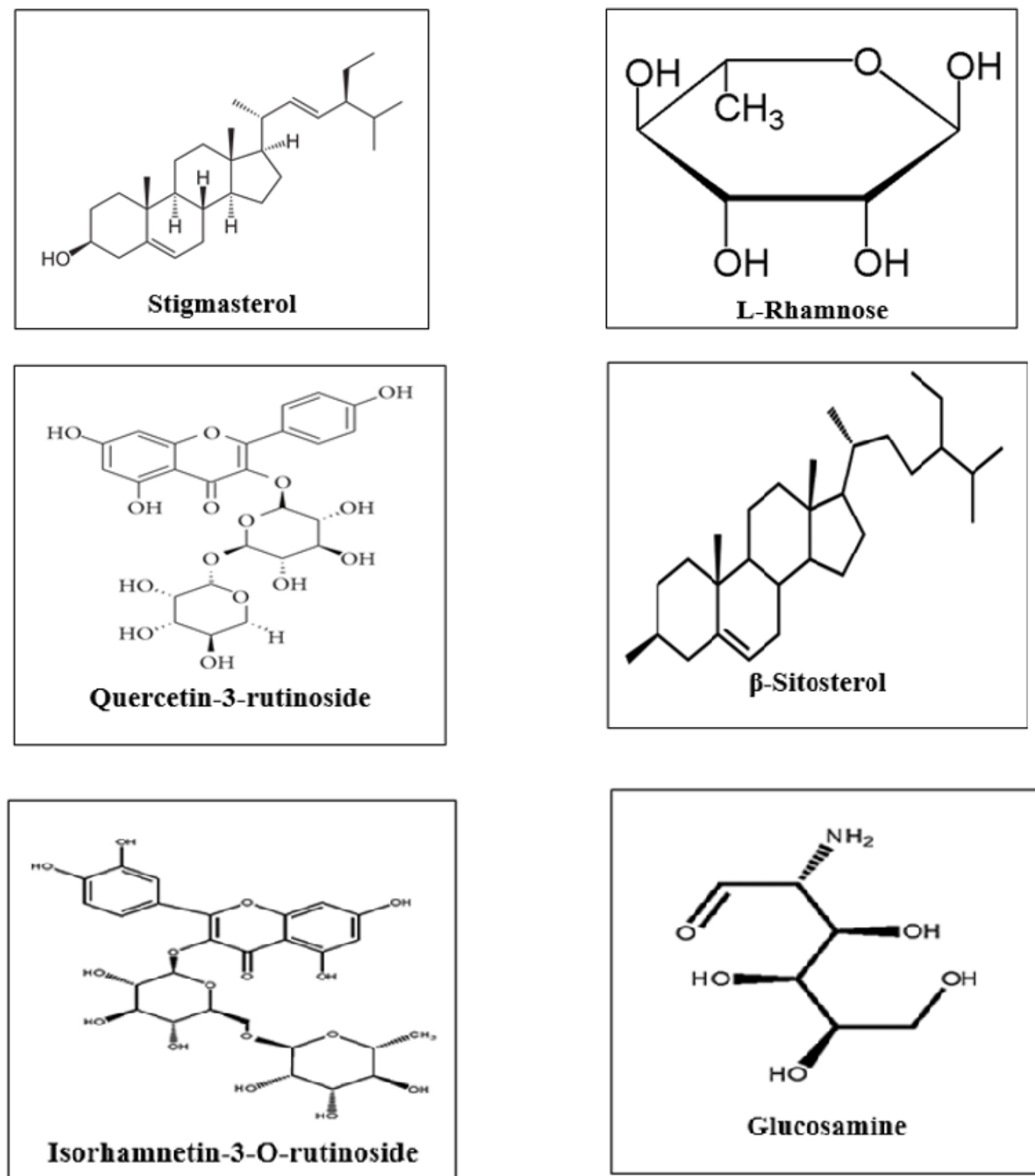


Figure 1: Structure of various phytochemical of *C. procera*

Varieties of Nanoparticles Synthesized using *C. procera*

Various nanoparticles such as silver, gold, copper, copper oxide, zinc oxide, iron oxide, magnetite, cerium oxide, and titanium dioxide have been synthesized using different parts of *Calotropis procera*, including leaves, latex, flowers, and roots. The different types of nanoparticles derived from the plant are illustrated in the accompanying (Figure 2).

Silver Nanoparticle (AgNPs)

Silver Nanoparticles (AgNPs) are among the most widely studied nanomaterials due to their unique and desirable characteristics. These include excellent conductivity, chemical stability, catalytic efficiency, enhanced Raman effects, and antimicrobial activity, attracting significant research interest across disciplines.^[32] Various parts of the *C. procera* plant have been utilized for the synthesis of Silver Nanoparticles (AgNPs), each demonstrating distinct pharmacological activities. Maisam *et al.*, (2025) reported the green synthesis of Silver Nanoparticles (AgNPs) ranging in size from 30 to 130 nm using aqueous extracts from the flowers and latex of *C. procera*. The antibacterial potential of these biosynthesized AgNPs was evaluated through an *in vitro* study against *Escherichia coli*, *Bacillus subtilis*, *Staphylococcus aureus*, and *Pseudomonas aeruginosa*, using varying concentrations of 100, 125, 150, 200, 250, and 500 µL. The results demonstrated a clear dose-dependent response, with higher concentrations leading to increased inhibition zones. These findings highlight the effectiveness of *C. procera*-mediated AgNPs as antibacterial agents, with a strong correlation between nanoparticle concentration and antimicrobial activity.^[33] Other studies also highlighted the green synthesis of Silver Nanoparticles (AgNPs) using *C. procera*, demonstrating their potential for a wide range of therapeutic applications. The biosynthesized AgNPs exhibited notable activities, including anti-diabetic, antioxidant, anti-inflammatory,^[34] hepatoprotective,^[35] anticancer,^[36] immunomodulatory,^[37] and larvicidal effects. This eco-friendly approach not only supports sustainable nanoparticle production but also underscores the multifunctional biomedical potential of *C. procera*-mediated AgNPs.^[38]

Gold Nanoparticles (AuNPs)

Gold nanoparticles have gained significant interest among various metallic nanoparticles due to their exceptional properties and broad applicability, particularly in the fields of medicine and biology.^[39] Their high biocompatibility,^[40] adjustable surface plasmon resonance,^[41] minimal toxicity,^[42] and strong optical scattering and absorption capabilities make them ideal candidates for biomedical applications.^[43]

In a study conducted by Shittu and Stephen (2016), gold nanoparticles (AuNPs) with an average size of 45 nm were synthesized using an aqueous leaf extract of *C. procera* and

evaluated for their cytotoxic activity against the MCF-7 breast cancer cell line through an *in vitro* MTT assay. The results demonstrated a clear dose-dependent cytotoxic effect, where increasing concentrations of AuNPs led to a progressive decline in cell viability. Notably, the IC₅₀ value was determined to be 0.312 mg/mL, indicating significant antiproliferative potential of the plant-mediated AuNPs against cancer cells. This study highlights the promising application of *C. procera*-derived gold nanoparticles in cancer nanomedicine.^[44]

The study also reported that the biosynthesized AuNPs using *C. procera* exhibited notable antimicrobial, antioxidant, and antihypertensive activities, suggesting their multifunctional therapeutic potential. These findings underline the versatility of *C. procera*-mediated gold nanoparticles as promising agents for biomedical applications.^[45]

Zinc Oxide Nanoparticles (ZnONPs)

Zinc oxide Nanoparticles (ZnONPs) have attracted significant research interest for their roles in catalysis, gas sensing, and biomedical applications.^[46,47] Furthermore, ZnO nanoparticles are considered cost-effective and safe; the U.S. FDA has classified zinc oxide as a GRAS (Generally Recognized As Safe) metal oxide.^[48] In a recent *in vivo* study by Sharma *et al.*, (2025), zinc oxide nanoparticles (ZnO NPs) with an average size of 18.20 nm were synthesized using an aqueous leaf extract of *C. procera* and evaluated for their efficacy against root-knot nematodes (*Meloidogyne incognita*) in bitter melon plants. The nanoparticles were applied at varying concentrations, and the results revealed a significant improvement in plant growth parameters along with a reduction in nematode infestation. These findings highlight the potential of *C. procera*-mediated ZnO nanoparticles as a sustainable and effective nanobiocontrol agent in agricultural pest management.^[49] In addition to their nematocidal effect, other studies have also reported that *C. procera*-derived nanoparticles exhibit strong antimicrobial, antioxidant, and anticancer activities, underscoring their multifunctional potential in both agricultural and biomedical applications.^[50,51]

Copper oxide nanoparticles (CuONPs)

K. Rayapa Reddy reported the green synthesis of CuO nanoparticles using *C. procera*, a plant belonging to the Asclepiadaceae family. These nanoparticles, characterized by their narrow band gap, have found widespread application in various fields, particularly in catalysis and photocatalytic processes.^[52,53] CuO nanoparticles (CuONPs) synthesized using *C. procera* leaf extract demonstrated strong adsorption capacity for Cr(VI), indicating their potential as an effective and eco-friendly alternative for removing hexavalent chromium from aqueous environments.^[54] Sethupandian *et al.*, (2023) demonstrated the green synthesis of Copper Oxide (CuO) nanoparticles using an aqueous seed extract of *C. procera*. The biosynthesized CuO nanoparticles were evaluated for their antibacterial activity through *in vitro*

assays against both Gram-positive (*Staphylococcus aureus*) and Gram-negative bacteria, including *Escherichia coli*, *Pseudomonas aeruginosa*, *Vibrio cholerae*, and *Aeromonas hydrophila*. The results revealed significant antibacterial efficacy, with the nanoparticles exhibiting inhibitory effects against all tested bacterial strains, indicating the broad-spectrum antimicrobial potential of *C. procera*-mediated CuO nanoparticles. These findings suggest their promising application in controlling bacterial pathogens through environmentally friendly nanomaterials.^[55]

Copper nanoparticles (CuNPs)

Copper nanoparticles have made remarkable advancements in the fields of nanotechnology and nanomedicine over the past decade, owing to their outstanding catalytic, optical, electrical, antifungal and antibacterial properties.^[56] Copper nanoparticles (Cu NPs) were synthesized through a green approach by Harne *et al.*, (2012) using an aqueous latex extract of *C. procera* and investigated their biocompatibility through *in vitro* studies on three different cell lines. The results revealed that Cu NPs exhibited excellent cell viability across all tested concentrations. This suggests that the copper nanoparticles synthesized using *C. procera* latex possess high biocompatibility, making them promising candidates for biomedical applications. While the study did not show direct anticancer activity, the demonstrated safety profile of these nanoparticles supports their potential use as nanocarriers or in combination therapies for cancer treatment.^[57]

Cerium oxide (CeO₂) nanoparticles

Cerium oxide (CeO₂) is a semiconductor metal oxide characterized by a band gap energy of approximately 3.19 eV and is widely used in bioimaging, catalysis, antibacterial applications, and sunscreens formulations, with various synthesis methods underscoring its industrial and biomedical relevance.^[58] Muthuvel *et al.*, (2020) reported the green synthesis of cerium oxide nanoparticles (CeO₂-NPs) using an aqueous flower extract of *C. procera*, resulting in nanoparticles with an average size of 21 nm. The antibacterial activity of the synthesized CeO₂-NPs was evaluated *in vitro* against both Gram-positive (*Bacillus subtilis*, *Staphylococcus saprophyticus*) and Gram-negative (*Escherichia coli*, *Pseudomonas aeruginosa*) bacterial strains at concentrations ranging from 5 to 100 µg/mL. At the highest tested concentration, the nanoparticles exhibited strong antibacterial efficacy against all microorganisms. These findings highlight the potent broad-spectrum antibacterial potential of *C. procera*-mediated CeO₂ nanoparticles, making them promising candidates for antimicrobial applications.^[59]

Iron oxide nanoparticles (FeONPs)

Ali *et al.*, (2020) synthesized iron oxide nanoparticles (~32 nm in size) using an aqueous leaf extract of *C. procera* and evaluated their antifungal activity through an *in vitro* study against *Alternaria*

alternata. The nanoparticles were tested at various concentrations (0.1 to 1.0 mg/mL). The highest concentration showed the most effective fungal inhibition, with a growth suppression rate of 81.9%, which was nearly equivalent to that of a standard chemical fungicide (82.2%). These results suggest that *C. procera*-mediated iron oxide nanoparticles are not only effective but could serve as an eco-friendly alternative to conventional fungicides in managing plant fungal pathogens.^[60]

Titanium oxide nanoparticles (TiO₂ NPs)

Titanium dioxide (TiO₂) nanoparticles have attracted widespread interest due to their remarkable antibacterial and antifungal properties, effective ultraviolet (UV) light filtering capabilities, and exceptional catalytic and photochemical performance. These multifunctional characteristics make them highly valuable for various industrial, environmental, and biomedical applications.^[61-63] In a recent study, Fatima *et al.*, (2025) synthesized titanium dioxide nanoparticles (TiO₂ NPs) using an aqueous latex serum extract of *C. procera* and evaluated their insecticidal activity against different developmental stages (2nd and 4th instar nymphs and adults) of the dusky cotton bug (*Oxycarenus* spp.). The study demonstrated a strong dose-dependent insecticidal effect, with the highest mortality rates observed in second instar nymphs (90-95%) and the lowest in adults (around 70%). Overall, the TiO₂ nanoparticles achieved up to 95% control of the insect population, indicating that *C. procera*-mediated TiO₂ NPs are highly effective as a botanical nanoinsecticide, particularly against early-stage pests.^[64]

Magnetite nanoparticles (Fe₃O₄ NPs)

Magnetite nanoparticles (Fe₃O₄) have attracted considerable scientific attention owing to their excellent biocompatibility, low cytotoxicity, simple synthesis methods, and eco-friendly biodegradability.^[65] Kalu *et al.*, (2022) reported the green synthesis of magnetite nanoparticles, with sizes ranging from 62.83 to 134 nm, using an aqueous leaf extract of *C. procera*. The antimicrobial potential of these nanoparticles was assessed *in vitro* at a concentration of 100 mg/mL against some microorganisms, including two Gram-positive bacteria (*Staphylococcus aureus* and *Bacillus subtilis*), two Gram-negative bacteria (*Escherichia coli* and *Klebsiella pneumoniae*), and two fungal strains (*Aspergillus niger* and *Fusarium oxysporum*). The nanoparticles exhibited notable inhibition against Gram-positive bacterial and fungal strains, while showing limited activity against Gram-negative bacteria. These findings suggest the potential of *C. procera*-mediated magnetite nanoparticles as effective agents against specific bacterial and fungal pathogens. Moreover, the eco-friendly and cost-effective green synthesis approach offers a promising alternative for developing magnetite-based nanomaterials, encouraging further studies focused on their optimization, mechanism of action, and application in biomedical and agricultural fields.^[66]

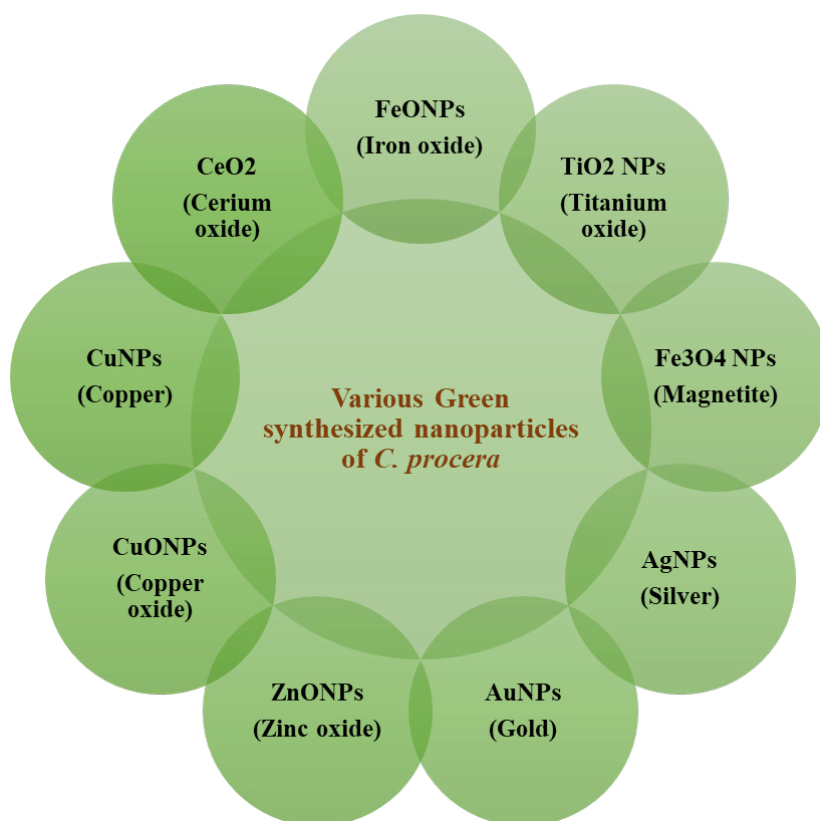


Figure 2: Different types of Nanoparticles of *C. procera*.

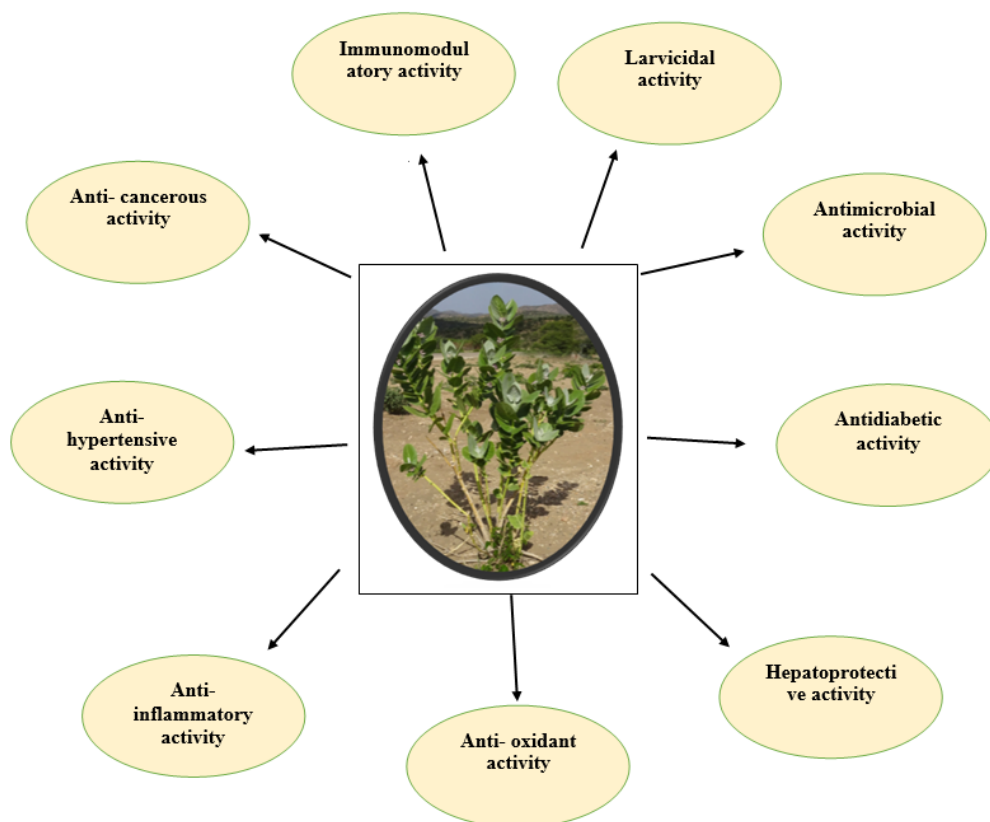


Figure 3: Different pharmacological activities of *C. procera*.

Pharmacological activity of nanoparticles synthesized using *C. procera*

Calotropis procera-mediated nanoparticles have been extensively studied for their broad spectrum of pharmacological properties, attributed to the plant's abundance of bioactive compounds. Various nanoparticles synthesized from different parts of the plant-such as leaves, roots, latex, and flowers-have demonstrated significant therapeutic potential. These include anti-inflammatory, antimicrobial, antioxidant, anticancer, antidiabetic, antihypertensive, immunomodulatory, and larvicidal activities. The key pharmacological activities are summarized in Table 1, which presents details including the year of publication, type and

size of nanoparticles, plant part and extract used, dosage, mode of administration, duration of treatment, experimental model, and observed effects.

Various pharmacological activities have been illustrated in Figure 3.

POSSIBLE MECHANISMS OF VARIOUS PHARMACOLOGICAL ACTIVITIES

Figure 4 presents a comprehensive summary of the underlying mechanisms responsible for the various pharmacological activities described in Table 1, offering a visual representation to enhance understanding of their mode of action.

Table 1: Various pharmacological activities of Green synthesized nanoparticles using *C. procera*.

| | Name of Nanoparticles/size | Part Used | Type of plant extract | Animal model | Dose duration and route | Observation and results | References |
|------------------------|----------------------------|-------------------|-----------------------|---|---|---|------------|
| Antimicrobial activity | AgNPs/ 30 to 130 nm | Flowers and Latex | Aqueous extract | <i>In vitro</i> study against <i>E. coli</i> , <i>B. subtilis</i> , <i>S. aureus</i> , and <i>P. aeruginosa</i> . | 100, 125, 150, 200, 250 and 500 μ L | The antibacterial activity of the nanoparticles was dose-dependent, with higher concentrations resulting in greater inhibition across all tested bacterial strains. For <i>P. aeruginosa</i> , the lowest inhibition zone of 10.5 mm was observed at 100 μ L, while the highest inhibition zone of 21.5 mm was recorded at 500 μ L. For <i>B. subtilis</i> , the inhibition zone was observed minimum of 17 mm at 100 μ L and maximum of 28 mm at 500 μ L. For <i>S. aureus</i> , the smallest inhibition zone was 19.5 mm at 100 μ L, increasing to 25 mm at 500 μ L. For <i>E. coli</i> , the inhibition zone was found 12.5 mm at 100 μ L and maximum of 25 mm at 500 μ L. | [33] |
| | AgNPs/ 29-46 nm | Leaves | Aqueous extract | <i>In vitro</i> study against Gram-positive (<i>B. subtilis</i> , <i>B. megaterium</i>) and Gram-negative (<i>S. flexneri</i>) bacteria and against the fungi (<i>T. viride</i> , <i>P. crysogenum</i> , and <i>A. niger</i>) | 100 μ L | The zone of inhibition results demonstrated by AgNPs revealed antibacterial activity against <i>B. megabacterium</i> (18 ± 1.89 mm), <i>B. subtilis</i> (20 ± 1.95 mm), and <i>S. flexneri</i> (21 ± 1.99 mm). Antifungal activity was also observed, with inhibition zones against <i>A. niger</i> (22 ± 2.14 mm), <i>P. chrysogenum</i> (20 ± 1.98 mm), and <i>T. viride</i> (18 ± 2.16 mm). | [34] |

| | | | | | | | |
|--|-------------------------|--------------------------------|--------------------|---|---|---|------|
| | AuNPs | Leaves | Aqueous extract | <i>In vitro</i> study against fungal strain <i>A. niger</i> , <i>A. flavus</i> , <i>F. poae</i> , <i>F. solani</i> and <i>P. avenatum</i> | 150 μ L/ mL | The AuNPs exhibited notable antifungal activity at a concentration of 150 μ L/mL, showing mycelial inhibition rates of 70.0%, 60.0%, 60.4%, 72.2%, and 82.0% against <i>F. solani</i> , <i>F. poae</i> , <i>A. niger</i> , <i>A. flavus</i> , and <i>P. avenatum</i> , respectively, when compared to the mycelial growth observed in the control group. | [45] |
| | AgNPs/ 15.30 - 17.66 nm | Leaves | Aqueous extract | <i>In vitro</i> study against <i>P. aeruginosa</i> , <i>E. sichuanensis</i> , <i>E. coli</i> , <i>S. aureus</i> , <i>S. agalactiae</i> | 10 and 20 μ L | The synthesized AgNPs exhibited potent antibacterial activity, as evidenced by the zones of inhibition observed against various bacterial strains: <i>E. coli</i> (18.1 \pm 0.2 mm), <i>E. sichuanensis</i> (16.8 \pm 0.5 mm), <i>P. aeruginosa</i> (14.4 \pm 0.3 mm), <i>S. aureus</i> (22.2 \pm 0.5 mm), and <i>S. agalactiae</i> (21.5 \pm 0.1 mm). | [67] |
| | AuNPs /41.88 nm | Leaves, root, stem, and flower | Methanolic extract | <i>In vitro</i> study against <i>S. larcymans</i> (fungal strain) | 5, 10, 15, 20, 30, 40 and 50 μ L | AuNPs of plant extract exhibited antifungal activity by producing a zone of inhibition measuring 3.2 mm at a concentration of 50 μ L, 3.0 mm at 40 μ L, and 2.1 mm at 30 μ L. | [68] |
| | ZnO NPs/ 100-200 nm | Leaves | Aqueous extract | <i>In vitro</i> study against human pathogenic bacteria <i>E. coli</i> , <i>P. aeruginosa</i> , <i>K. pneumoniae</i> , <i>S. aureus</i> and plant isolated bacteria <i>X. axonopodis</i> . Fungal strain- <i>Aspergillus</i> sps. and <i>Penicillium</i> sps. | 10, 20 and 30 μ L for bacteria 100, 200 and 300 μ L for fungal strain | The green-synthesized ZnO nanoparticles demonstrated potent antibacterial activity against both human and plant pathogens at all tested concentrations. The highest zone of inhibition was observed at the 30 μ L concentration. Interestingly, as the concentration of ZnO nanoparticles increased beyond 30 μ L, a reduction in the inhibition zone was noted. Thus, the maximum antibacterial effect was achieved at 30 μ L. According to the MIC data, complete inhibition of all tested microorganisms was achieved at concentrations ranging from 50 to 12.5 μ g/mL of nano-ZnO. The antifungal assay results indicated that all concentrations of ZnO nanoparticles significantly inhibited spore germination. | [51] |

| | | | | | | | |
|--|------------------------------|------------------------|-----------------|--|-------------------------|--|------|
| | AgNPs | Latex from young twigs | - | <i>In vitro</i> study against <i>S. aureus</i> , <i>E. coli</i> , <i>E. coccus</i> , <i>E. faecalis</i> , <i>P. aeruginosa</i> and <i>K. pneumonia</i> bacterial strain. | 10-100µg/mL | L-AgNPs displayed potent and concentration-dependent antibacterial activity against a variety of pathogenic microorganisms. The degree of microbial inhibition varied significantly among the different tested bacterial strains. The antibacterial effect was significantly more prominent against Gram-negative organisms compared to Gram-positive ones. | [38] |
| | CuONPs1/20-50 nm | Seed | Aqueous extract | <i>In vitro</i> study against gram positive bacteria (<i>E. coli</i> , <i>S. aureus</i>) and gram negative bacteria (<i>P. aeruginosa</i> , <i>Vibrio cholera</i> and <i>A. hydrophila</i>) | - | The green synthesized CuONPs exhibited strong toxicity against various pathogenic bacterial species and showed antibacterial activity against all tested bacterial strains. The zones of growth inhibition were observed in the following decreasing order: <i>V. cholerae</i> , <i>E. coli</i> , <i>P. aeruginosa</i> , <i>S. aureus</i> , and <i>A. hydrophila</i> . | [55] |
| | AgNPs/ 20-30 nm | Leaves and Flowers | Aqueous extract | <i>In vitro</i> study against <i>Streptococcus</i> spp, <i>Salmonella</i> spp, <i>E. coli</i> , and <i>S. aureus</i> | 0.1, 0.25 and 0.5 mg/mL | The antimicrobial potential of C.p-AgNPs was investigated and found to exhibit dose-dependent inhibition. At 0.25 and 0.5 mg/mL, AgNPs effectively inhibited bacterial growth, yielding inhibition zones of 12 mm and 16 mm for <i>E. coli</i> , 7 mm and 12 mm for <i>S. aureus</i> , 10 mm and 13 mm for <i>Streptococcus</i> , and 9 mm and 14 mm for <i>Salmonella</i> spp., respectively. | [69] |
| | AgNPs/average sizes 14-25 nm | Stem | Aqueous extract | <i>In vitro</i> study against bacterial isolates such as <i>E. coli</i> , <i>P. aeruginosa</i> , <i>B. cereus</i> and <i>S. aureus</i> and against some pathogenic fungi; <i>F. oxysporum</i> , <i>Rhizopus</i> sp. <i>A. niger</i> and <i>A. flavus</i> | - | The inhibition zones were observed for <i>E. coli</i> (12 mm), <i>P. aeruginosa</i> (19 mm), and <i>B. cereus</i> (29 mm), while <i>S. aureus</i> showed no susceptibility. In antifungal activity, <i>A. niger</i> exhibited a 14 mm zone of inhibition, whereas <i>F. oxysporum</i> , <i>Rhizopus</i> sp., and <i>A. flavus</i> showed no observable inhibition. | [70] |

| | | | | | | | |
|--|--|--------|-----------------|--|---------------------------------|--|------|
| | Fe ₃ O ₄ NPs/62.83- 134 nm | Leaves | Aqueous extract | <i>In vitro</i> study against two Gram-positive bacteria (<i>S. aureus</i> and <i>B. subtilis</i>), two Gram-negative bacteria (<i>E. coli</i> and <i>K. pneumoniae</i>), and two fungal strains (<i>A. niger</i> and <i>F. oxysporum</i>). | 100 mg/mL | The antimicrobial efficacy was demonstrated by inhibition zones ranging from 7.1 mm to 22.5 mm against <i>K. pneumoniae</i> , <i>S. aureus</i> , <i>B. subtilis</i> , <i>A. niger</i> , and <i>F. oxysporum</i> , whereas no inhibitory effect was detected against <i>E. coli</i> . The results of this study also revealed that the antimicrobial activity against Gram-positive bacteria was significantly higher compared to the other tested microorganisms, while the activity against fungal isolates was significantly greater than that observed against Gram-negative bacteria | [66] |
| | ZnO NPs/ 25.7 nm | Leaves | Aqueous extract | <i>In vitro</i> study against bacteria <i>E. coli</i> , <i>E. fecalicus</i> , <i>Klebsiella</i> sp., <i>Salmonella</i> sp., <i>streptococcus pyogens</i> , <i>S. aureus</i> , <i>Proteus</i> sp., <i>Pseudomonas</i> sp., and fungal strain <i>C. albicans</i> . | 40, 80, and 120 µL | The study revealed that varying concentrations of green-synthesized ZnO nanoparticles exhibited notable antimicrobial sensitivity, with the maximum zone of inhibition observed at the concentration of 120 µg/mL. In the antifungal study, the ZnO nanoparticles exhibited the greatest inhibition at the highest concentration tested. | [71] |
| | Zno NPs/ 12.08 nm | Leaves | Aqueous extract | <i>In vitro</i> study against <i>E. coli</i> | - | The green-synthesized nanoparticles significantly enhanced the antimicrobial effect, increasing the inhibition zone to 49% | [72] |
| | CP-AgNPs/ 28.72 nm | - | Latex | <i>In vitro</i> study against <i>P. aeruginosa</i> , <i>K. pneumoniae</i> , <i>S. aureus</i> and <i>B. subtilis</i> | 64, 32, 16, 8, 4, 2 and 1 µg/mL | The MIC of CP-AgNPs was found to be 4 µg/mL against <i>P. aeruginosa</i> and <i>B. subtilis</i> , and 8 µg/mL against <i>K. pneumoniae</i> and <i>S. aureus</i> . The MBC for all tested bacterial strains was determined to be 32 µg/mL. CP-AgNPs inhibited biofilm formation by all four bacterial strains by approximately 80%. | [73] |

| | | | | | | | |
|--|---------------------------|---------|-----------------|---|----------------------------|--|------|
| | AgNPs/10nm | - | - | <i>In vitro</i> study against <i>S. aureus</i> , MRSA, <i>S. typhimurium</i> and <i>E. coli</i> | 1.6 to 4 mg | The bacterial inhibition was concentration-dependent. AgNPs exhibited antibacterial activity, with inhibition zone values ranging from 8 to 10 mm against <i>S. aureus</i> and MRSA, and from 7 to 9 mm against <i>S. typhimurium</i> and <i>E. coli</i> . | [74] |
| | AgNPs/ 70- 80 nm | Flowers | Aqueous extract | <i>In vitro</i> study against <i>S. aureus</i> and <i>P. acnes</i> . | 10, 15, 20, 25 and 30 µg/g | <i>S. aureus</i> exhibited the highest zone of inhibition (13.5±1 mm), while <i>P. acnes</i> showed (8±1 mm). The bacterial strains displayed no resistance to the flower extract control and showed only a minimal inhibitory response to the silver nitrate control. | [36] |
| | AgNPs and honey/ 60-85 nm | Leaves | Aqueous extract | <i>In vitro</i> study against Gram positive (<i>S. aureus</i> and <i>B. subtilis</i>) and Gram negative (<i>P. mirabilis</i> and <i>E. coli</i>) bacteria. | 20% AgNPs and 20% honey | AgNPs demonstrated effective antimicrobial activity by inhibiting the growth of both bacterial and fungal pathogens. The maximum zone of inhibition was observed against <i>Bacillus subtilis</i> (29±0.040 mm), while the minimum inhibition was recorded against <i>Micrococcus luteus</i> and <i>K. pneumoniae</i> (19±0.037 mm). | [37] |
| | AgNPs/ 38-44 nm | Roots | Aqueous extract | <i>In vitro</i> study against <i>S. typhi</i> , <i>S. flexneri</i> , <i>B. subtilis</i> , <i>E. coli</i> , <i>S. aureus</i> , <i>Enterococcus</i> sp., <i>K. pneumoniae</i> , <i>P. aeruginosa</i> , <i>S. epidermidis</i> , and <i>E. faecalis</i> . | 10, 25, 50 and 100 µg | Among all the tested pathogenic bacterial strains, <i>S. flexneri</i> , <i>E. coli</i> , <i>P. aeruginosa</i> , and <i>E. faecalis</i> exhibited the highest sensitivity towards AgNPs, as evidenced by their lowest observed MIC value of 3.12 µg/mL. <i>S. typhi</i> and <i>B. subtilis</i> also showed considerable susceptibility to AgNPs, with an MIC value of 6.25 µg/mL, suggesting moderate antibacterial activity. On the other hand, a relatively higher degree of resistance was recorded for <i>S. aureus</i> , <i>Enterococcus</i> species, <i>K. pneumoniae</i> , and <i>S. epidermidis</i> , which demonstrated reduced sensitivity by exhibiting a MIC value of 12.5 µg/mL. | [75] |

| | | | | | | | |
|--|---|--------|-----------------|--|------------------------------------|---|------|
| | FeO NPs/32 nm | Leaves | Aqueous extract | <i>In vitro</i> study against fungi <i>A. alternata</i> . | 1.0, 0.75, 0.5, 0.25 and 0.1 mg/mL | A concentration of 1.0 mg/mL showed the highest and most comparable level of effectiveness. At this concentration, iron oxide nanoparticles and chemical fungicides exhibited growth inhibition rates of 81.9% and 82.2%, respectively. Interestingly, at lower concentrations, the nanoparticles demonstrated even greater inhibitory effects than the chemical fungicide. | [60] |
| | CeO ₂ -NPs/ average size 21 nm | Flower | Aqueous extract | <i>In vitro</i> study against Gram positive (<i>B. subtilis</i> , <i>S. saprophyticus</i>) and Gram negative (<i>E. coli</i> , <i>P. aeruginosa</i>). | 5, 10, 20, 40, 80 and 100 µg/mL | The biosynthesized CeO ₂ nanoparticles exhibited strong antibacterial activity against all tested microorganisms at a concentration of 100 µg/mL. The observed zones of inhibition were 23±0.48 mm for <i>E. coli</i> , 21±0.84 mm for <i>P. aeruginosa</i> , 21±0.78 mm for <i>S. saprophyticus</i> , and 20±0.41 mm for <i>B. subtilis</i> | [59] |
| | Latex silver nanoparticles (LAg-NPs)/ 2.26-30 nm. | Leaves | Latex | <i>In vitro</i> study against Gram-negative bacteria (<i>E. coli</i> and <i>P. aeruginosa</i>), Gram-positive bacteria (<i>S. aureus</i> and <i>B. subtilis</i>) and fungal strains of (<i>C. albicans</i> and <i>A. niger</i>). | 25, 50, 75, 100 and 125 µg / mL | The silver nanoparticles exhibited varying degrees of growth inhibition across all tested strains. The largest inhibition zone was observed at the concentration of 125 µg/mL for all microorganism, indicating a concentration-dependent antimicrobial effect. | [4] |

| | | | | | | | |
|-----------------------|-------------------------------|--------|-----------------|--|--|---|------|
| | ZnO NPs/ 100-200 nm | Leaves | Aqueous extract | <i>In vitro</i> study against- Human pathogen (<i>E. coli</i> , <i>P. aeruginosa</i> , <i>K. pneumoniae</i> , <i>S. aureus</i>) -plant pathogenic organism (<i>X. axonopodis</i>) and -Fungal strain (<i>Penicillium</i> sps., <i>Aspergillus</i> sps.) | For bacteria- 10, 20 and 30 μ L For fungal-100 μ L, 200 μ L, and 300 μ L | For human pathogen- All tested microorganisms were completely inhibited at nano-ZnO concentrations ranging from 50 to 12.5 μ g/mL. The MIC of ZnO NPs showed the most effective inhibition against all tested bacteria at a concentration of 50 μ g/mL. For plant pathogen- ZnO nanoparticles exhibited the highest zones of inhibition, measuring 16 mm and 18 mm respectively, at a concentration of 30 μ g/mL against <i>X. axonopodis</i> . Interestingly, the zone of inhibition for plant pathogenic strains decreased with increasing concentrations of ZnO nanoparticle. For fungi- Various concentrations of ZnO nanoparticles resulted in significant inhibition. The greatest inhibition was observed at the highest concentration of nanoparticles. | [76] |
| | LAGNPs/ average size 12.33 nm | - | Latex serum | <i>In vitro</i> study against bacteria (<i>E. coli</i> , <i>P. aeruginosa</i> , <i>Serratia</i> sp.)- and fungi (<i>T. rubrum</i> , <i>C. albicans</i> , <i>A. terreus</i>) | -For bacteria 105, 10, 20 μ L- for fungi 10, 25, 50 μ L | The MIC of LAG-NPs was 5 μ L for <i>E. coli</i> , and 10 μ L for <i>Serratia</i> sp. and <i>P. aeruginosa</i> . Among the fungal strains, the MIC was 10 μ L for <i>C. albicans</i> , while <i>T. rubrum</i> and <i>A. terreus</i> found 25 μ L. | [77] |
| Antidiabetic activity | AgNPs/ 29-46 nm | Leaves | Aqueous extract | <i>In vitro</i> study | 250 μ L | The results showed that AgNPs demonstrated α -amylase inhibitory activity of $83.29 \pm 0.26\%$, significantly higher than the inhibition observed with metformin, which was $2.40 \pm 0.18\%$ at the same tested concentration. | [34] |

| | | | | | | | |
|---------------------------|---------------------|--------|--------------------|---|--|--|------|
| Hepatoprotective activity | CPL AgNPs/ 9- 48 nm | Leaves | Methanolic extract | <i>Plasmodium berghei</i> -Infected Liver in Mice | 10, 25 and 50 mg/kg, orally CPL AgNPs for 7 days | Administration of CPL- AgNPs to infected mice led to a marked reduction in parasitemia, (treated with 50 mg/kg CPL AgNPs showed < 3% parasitemia). CPL- AgNPs decrease the expression of hepatic cytokines, including IL-1 β and IL-10. The treatment of mice with CPL- AgNPs led to a reduction in the activities of ALP, AST, and ALT enzymes. Histopathological analysis revealed significant improvement in liver tissue architecture, hepatic lesions were notably reduced, liver damage score decreased and reduced infiltration of inflammatory cells. | [35] |
| Anti- oxidant activity | CPL- AgNPs/29-46 nm | Leaves | Aqueous extract | <i>In vitro</i> study | 50 μ L | The hydrogen peroxide scavenging assay revealed inhibition values of 29.31 \pm 0.21% for CPL- AgNPs and 0.13 \pm 0.19% for ascorbic acid, indicating that CPL- AgNPs possess significantly stronger scavenging activity. Furthermore, the reducing power assay confirmed that AgNPs exhibited a 4.38% reducing power activity, compared to 2.08% for the standard antioxidant BHT, even at very low concentrations. | [34] |
| | AgNPs | Leaves | Aqueous extract | <i>In vitro</i> study | 1, 2, 3, 4 and 5 mg/mL | The antioxidant activity of the AgNPs increased progressively with rising concentrations. The DPPH assay results demonstrated that both the synthesized AgNPs and the standard antioxidant effectively inhibited DPPH radicals. The synthesized AgNPs displayed a dose-dependent ABTS radical scavenging activity, though their effectiveness was comparatively lower than that of the standard antioxidants. The FRAP assay revealed their ability to donate electrons. This reducing capacity increased with rising concentrations; however, it was still lower compared to that of the standard antioxidants. | [78] |

| | | | | | | | |
|-----------------------------|----------------------------------|--|-------------------------------------|--|--|--|------|
| | AuNPs | Leaves | Aqueous extract | <i>In vitro</i> study | 50, 100, 150 and 200 μ L/mL | The DPPH radical scavenging activity of the AuNPs was recorded as 89.66%, 84.23%, 81.09%, and 80.64% at concentrations of 50, 100, 150, and 200 μ L/mL, respectively. | [45] |
| | ZnO NPs and Fe NPs/ 32.67-202 nm | Aerial parts (stem, leaf, fruit, flower) | Aqueous and hydroalcoholic extracts | <i>In vitro</i> study (A-431 cell lines) | 10, 20, 40, 60, 80 and 100 μ L/ mL | Results from both ABTS and DPPH assays revealed that ZnO NPs showed the most effective scavenging activity against DPPH radicals (IC_{50} =148.46 μ g/mL), whereas FeNPs demonstrated comparatively lower activity. Conversely, FeNPs exhibited the highest ABTS radical scavenging potential (IC_{50} =52.81 μ g/mL), with ZnO NPs displaying slightly reduced efficacy in comparison. | [50] |
| | AgNPs/ 70- 80 nm | Flowers | Aqueous extract | <i>In vitro</i> study (A-431 cell lines) | 10, 15, 20, 25 and 30 μ g/ mL | The nanogel exhibited strong DPPH radical scavenging activity, with its antioxidant potential ranging from 38% to 87.49% across concentrations of 10 to 30 μ g/g. The DPPH assay further confirmed that the nanogel formulation possessed superior antioxidant efficacy, showing an IC_{50} value of 14.94 ± 0.59 μ g/mL, which was more potent than that of ascorbic acid (IC_{50} = 32.24 ± 0.62 μ g/mL). | [36] |
| Anti- inflammatory activity | AgNPs/29-46 nm | Leaves | Aqueous extract | <i>In vitro</i> study | - | AgNPs showed anti-inflammatory activity with inhibition of albumin denaturation (%) of 2.08 ± 0.08 (%) which was compared with standard aspirin at 2.54 ± 0.11 (%). | [34] |
| | AgNPs | Latex from young twigs | - | <i>In vitro</i> study | 20, 40, 60, 80 and 100 μ g/ mL | The green-synthesized nanoparticles demonstrated significant inhibition of red blood cell (RBC) lysis. <i>In vitro</i> anti-inflammatory evaluations showed that the membrane-stabilizing potential of L-Ag NPs (82.73%) was comparable to that of the reference drug Aceclofenac (75.16%). Furthermore, the proteinase inhibition exhibited by L-Ag NPs (84.06%) and Aceclofenac (81.90%). | [38] |

| | | | | | | | |
|----------------------------|----------------------------------|--|---|---|---|--|------|
| Anti-hypertensive activity | AuNPs | Leaves | Aqueous extract | <i>In vitro</i> study | 50, 100, 150 and 200 µg/mL | The results demonstrate that the nanoparticles were more effective at a lower concentration (80.71±13.91% inhibition) and less effective at high concentration (37.84±0.09064%) in inhibiting Angiotensin I-converting enzyme activity. This study proposes that a lower concentration of the nanoparticles could be an effective option for managing hypertension | [45] |
| Anti- cancerous activity | ZnO NPs and Fe NPs/ 32.67-202 nm | Aerial parts (stem, leaves, fruits, flowers) | Aqueous and hydroalcoholic extracts | <i>In vitro</i> study (A-431 cell lines) | up to 1000 µg/mL | The results highlight the effectiveness of CP aqueous extract-mediated nanoparticles, with CZnQ emerging as the most potent candidate against the tested cell lines. After 72 hr of exposure, CZnQ significantly reduced cancer cell viability to 0.61% at a concentration of 1000 µg/mL, with an IC ₅₀ value of 188.97 µg/mL. | [50] |
| | AgNPs | Fresh leaves and flowers | Hot water extract, Acetone extract and Chloroform Extract | <i>In vitro</i> study Dalton's Lymphoma Ascites cells (DLA) | 12.5, 25, 50, 100 and 200 µL/ mL | These results indicate a dose-dependent correlation between AgNP concentration and cytotoxicity. An increase in AgNP concentration leads to a higher percentage of cell death, demonstrating that the nanoparticles become more toxic to cells at elevated doses. | [79] |
| | AgNPs/ 70- 80 nm | Flowers | Aqueous extract | <i>In vitro</i> study (A-431 cell lines) | 10, 15, 20, 25 and 30 µg/g | A progressive decline in cell viability was detected with increasing concentrations of nanogel, ranging from 10 to 30 µg/g, suggesting a dose-dependent cytotoxic effect. The IC ₅₀ values for the standard compound (Doxorubicin) and the nanogel were determined to be 27.74 µg/mL and 23.88 µg/mL, respectively. | [36] |
| | AgNPs/ 38-44 nm | Roots | Aqueous extract | <i>In vitro</i> study HEPK (Keratinocytes) cells | 0.78, 1.56, 3.125, 6.25, 12.5, 25, 50 and 100g/mL | The MTT assay results revealed that the AgNPs were non-toxic to mammalian cells compared to the positive control TNF-β, although cell viability decreased progressively with increasing concentrations. | [75] |

| | | | | | | | |
|---------------------|-------------------------------|--------|-----------------------|---|---|---|------|
| | AuNPs/ average 45 nm | Leaves | Aqueous extract | <i>In vitro</i> study (MCF-7cell line) | 0.156, 0.312, 0.625, 1.25, 2.5 and 5 mg/mL | The cytotoxicity results from the MTT assay demonstrated that cell viability declined progressively with increasing concentrations of gold nanoparticles, ranging from 0.156 mg/mL to 5 mg/mL. This dose-dependent reduction in cell viability resulted in a calculated IC ₅₀ value of 0.312 mg/mL. | [44] |
| | CuNPs | Latex | Aqueous extract | <i>In vitro</i> study (HeLa, A549 and BHK21 cell lines) | 0, 20, 40, 60, 80, 100, 120, 140 and 160 µM | Copper nanoparticles tested all three cell lines exhibited excellent cell viability even at concentrations up to 120 µM. The absence of cytotoxic effects in all three cell lines indicates that the copper nanoparticles synthesized using latex possess outstanding biocompatibility. | [57] |
| | AgNPs and honey/ 60-85 nm | Leaves | Aqueous extract | <i>In vitro</i> study (HeLa and HepG2cells) | 20% AgNPs and 20% honey | The combination of honey and AgNPs resulted in a reduced growth suppressive effect compared to honey alone. | [37] |
| Larvicidal activity | TiO ₂ NPs | Latex | Aqueous serum extract | Against 2 nd , 4 th instar nymphs and adult of dusky cotton bug (<i>Oxycarenus</i> spp.) | 600, 900, 1200, and 1500 ppm | The nanoparticles achieved up to 95% control of the insect population, with the highest effectiveness observed in second instar nymphs (between 90 and 95% mortality) and the lowest in adult stages (70% mortality). The total mortality percentage showed directly proportional to the concentration of the synthesized nanoparticles used. | [64] |
| | ZnO NPs/ average size18.20 nm | Leaves | Aqueous extract | Against Root-Knot Nematodes (<i>Meloidogyne incognita</i> affected bitter gourd plants) | 50, 100, 200, and 500 ppm | <i>In vivo</i> bioassay result showed that the treatment of bitter gourd plants affected by <i>M. incognita</i> with ZnO nanoparticles led to significant improvements in growth indices and a marked reduction in root gall formation. Plants treated with 500 ppm ZnO nanoparticles showed the most enhanced growth performance, including the highest shoot length (197.13 cm), root length (17.22 cm), fresh shoot weight (387.76 g), earliest flowering (29 days), and the lowest number of root galls (8.23), compared to control and other concentration groups. | [49] |

| | | | | | | | |
|--|--------------|-------------|-----------------|--|--------------------------------|--|------|
| | AgNPs/ 42 nm | young twigs | Latex | Against 4 th instar larvae of <i>Aedes aegypti</i> | 20, 40, 60, 80 and 100 µg/mL | The larval mortality rate of mosquitoes increased proportionally with the concentration of AgNPs. The lethal concentration (LC ₅₀) of L-AgNPs was determined to be 63.09 µg/mL. Morphological analysis showed that no external abnormalities were observed in the untreated larvae. However, larvae exposed to lower concentrations of AgNPs exhibited increased pigmentation and gut blackening. At higher concentrations, more severe effects were observed, including body shrinkage, disrupted and disorganized gut structure, and ruptured cuticle. | [38] |
| | ZnONPs | Leaves | Aqueous extract | Against second, third, fourth, fifth and sixth instar larvae of <i>Spodoptera frugiperda</i> | 100, 200, 300, 400 and 500 ppm | The first instar larvae exhibited the highest mortality rate of 85%, followed by 80%, 76%, 71%, 66%, and 55% for the second, third, fourth, fifth, and sixth instar larvae, respectively, at a concentration of 500 ppm. A decline in mortality frequency was observed with decreasing concentrations. ZnO nanoparticle treatment induced significant physical developmental abnormalities across all life stages-larvae, juveniles, and adults-in both males and females, disrupting normal body development and thereby contributing to the suppression of <i>S. frugiperda</i> populations. | [80] |
| | ZnONPs | Leaves | Aqueous extract | Against larvae of <i>Spodoptera litura</i> | 100, 200, 300 and 400 ppm | ZnO nanoparticles induced increasing levels of mortality across different concentrations-100, 200, 300, and 400 ppm-with the highest mortality observed at 400 ppm compared to the lower concentrations. No mortality was recorded in the control group. The LC ₅₀ was calculated to be 232.55 ppm, while the LC ₉₀ value was determined to be 530.81 ppm. Also, the weight of the pest showed a progressive decrease with increasing concentrations of the treatment. | [81] |

| | | | | | | | |
|---------------------------|-----------------|--------|-----------------|---|--|--|------|
| | AgNPs | Leaves | Aqueous extract | Against <i>Tribolium castaneum</i> pest | 0.714, 1.0, 1.28, 1.57 and 1.85 mg/cm ² | The study showed that AgNPs exhibited significant toxicity against <i>T. castaneum</i> , with the highest mortality observed at a concentration of 1.85 mg/cm ² , and there was no mortality observed in control group. These findings confirm that increase the concentration of AgNPs leads to a corresponding rise in <i>T. castaneum</i> mortality. | [82] |
| Immunomodulatory activity | AgNPs/ 60-85 nm | Leaves | Aqueous extract | <i>In vitro</i> study (Rat splenocytes) | 100 µg/mL | The MTT assay results indicated that AgNPs inhibited the proliferation of rat splenocytes. | [37] |

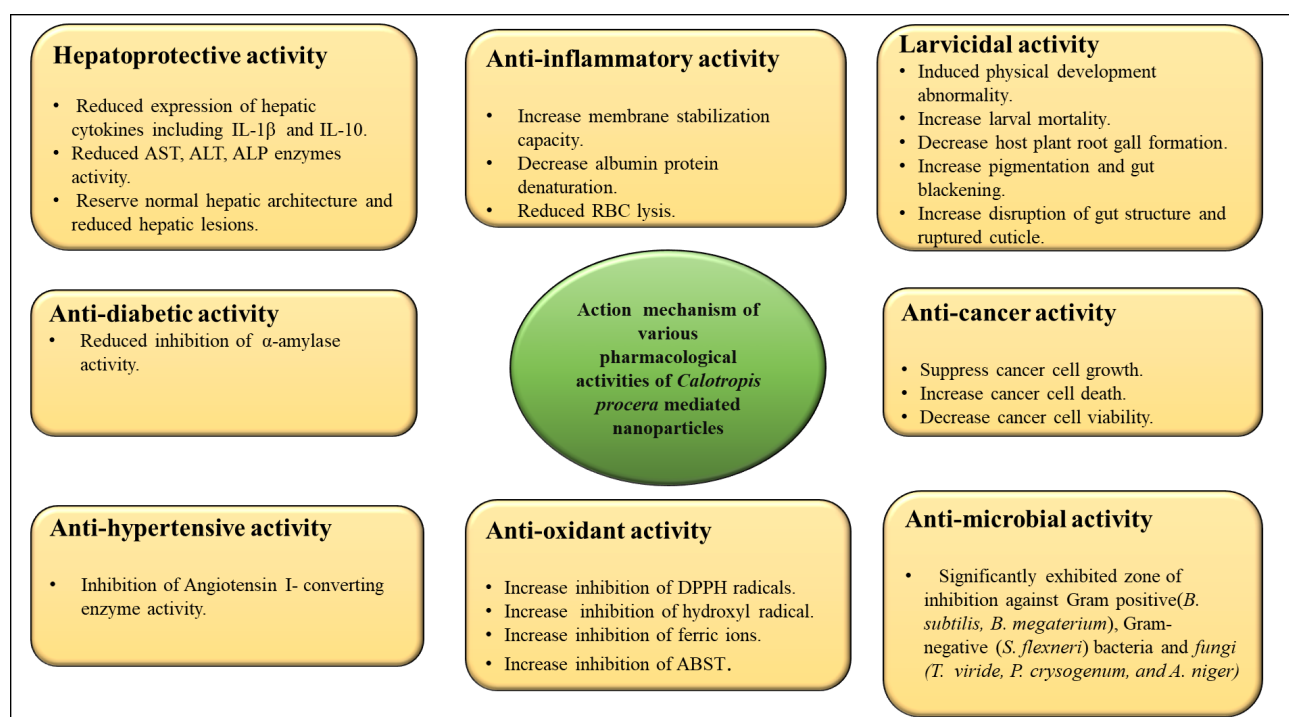


Figure 4: Mechanisms of Major pharmacological activities.

TOXICITY PROFILE

Assessing the toxicity profile is a vital step when exploring the medicinal potential of any plant, as it ensures safe and effective therapeutic use. Toxicological evaluations help identify possible adverse effects, determine lethal dose limits, and assess the overall risks linked to plant-derived compounds. *C. procera*, a widely recognized medicinal plant, contains a range of bioactive constituents that may offer therapeutic benefits but can also produce toxic effects, depending on the dosage and mode of administration. The latex of *C. procera* is recognized for its high toxicity. One study reported toxic effects in 29 individuals who accidentally came into contact with the latex through ocular exposure. These patients experienced sudden, painless vision loss accompanied by photophobia. Clinical observations revealed conjunctival congestion and varying levels of corneal

edema, along with the presence of Descemet's membrane folds in all cases.^[83-86] An acute toxicity study conducted on male rabbits using the up-and-down method estimated the LD₅₀ of *C. procera* leaf extract to be approximately 2435.25 mg/kg of body weight.^[27,87]

The study suggests that green-synthesized nanoparticles derived from *C. procera* could exhibit potential toxic effects, particularly at higher concentrations or with prolonged exposure. For example, *in vivo* study, ZnO and TiO₂ nanoparticles synthesized using *C. procera* were orally administered to albino mice at doses ranging from 100 to 300 mg/kg BW over a period of 7 to 21 days. The results revealed histopathological alterations in kidney tissues, indicating possible nephrotoxic effects. These findings suggest that while *C. procera*-mediated nanoparticles may possess desirable biological activities, their safety profiles require

careful evaluation.^[88] Further research is needed to assess organ effects, dosage impact, and long-term safety before using these nanoparticles in medical or environmental applications.

CONCLUSION

Calotropis procera is a widely recognized medicinal plant, long valued in traditional medicine for its diverse therapeutic applications. Nanoparticles synthesized using various parts of *C. procera*-including its leaves, roots, flowers, and latex-have shown significant pharmacological potential as promising agents for the development of novel, plant-based therapeutics. These green-synthesized nanoparticles, such as silver, zinc oxide, iron oxide, and gold nanoparticles, exhibit a broad spectrum of pharmacological activities, including antimicrobial, anti-inflammatory, antioxidant, anticancer, and larvicidal effects. However, the use of *C. procera* in nanoparticle synthesis raises toxicity concerns, primarily due to the presence of cardenolides and other toxic phytoconstituents. This review highlights the botanical profile, major phytochemical constituents, and traditional medicinal uses of *C. procera*, along with the various types of nanoparticles synthesized using this plant. It further explores the therapeutic applications and safety profile of *C. procera*-based nanoparticles, emphasizing their potential in the treatment of a wide range of health conditions. By compiling and critically analyzing the existing literature, this review provides valuable insights into the pharmacological activities and biological mechanisms of *C. procera*-derived nanoparticles. It underscores the need for detailed toxicological evaluations and clinical investigations to ensure their safe application. Ultimately, this review aims to support and guide future research toward the development of effective, biocompatible, and clinically relevant *C. procera*-based nanotherapeutics.

ACKNOWLEDGEMENT

We are thankful to Head, Department of Zoology, University of Rajasthan, Jaipur, for providing necessary facilities.

ABBREVIATIONS

LD₅₀: Lethal dose; **IC₅₀**: Inhibitory concentration; **TNF**: Tumor necrosis factor; **LC₅₀**: The lethal concentration; **IL**: Interleukin; **BW**: Body weight; **AST**: Aspartate Aminotransferase; **DPPH**: 2,2-Diphenyl-1-Picrylhydrazyl; **ALT**: Alanine Aminotransferase; **ALP**: Alkaline Phosphatase; **ABTS**: 2,2'-Azinobis(3-E thylbenzothiazoline-6-Sulfonic Acid); **FRAP**: Ferric Reducing Antioxidant Power; **MIC**: Minimum Inhibitory Concentration; **MBC**: Minimum Bactericidal Concentration; **IZ**: Inhibition Zone; **RBC**: Red Blood Cells; **E. coli**: *Escherichia coli*; **P. aeruginosa**: *Pseudomonas aeruginosa*; **E. faecalis**: *Enterococcus faecalis*; **S. typhimurium**: *Salmonella typhimurium*; **S. saprophyticus**: *Staphylococcus saprophyticus*; **S. aureus**: *Staphylococcus aureus*; **C. albicans**: *Candida albicans*; **B. subtilis**: *Bacillus subtilis*; **B.**

megaterium: *Bacillus megaterium*; **S. flexneri**: *Shigella flexneri*; **T. viride**: *Trichoderma viride*; **P. crysogenum**: *Penicillium crysogenum*; **P. mirabilis**: *Proteus mirabilis*; **K. pneumoniae**: *Klebsiella pneumoniae*; **F. poae**: *Fusarium poae*; **F. solani**: *Fusarium solani*; **P. avenatum**: *Penicillium avenatum*; **E. sichuanensis**: *Enterobacter sichuanensis*; **S. pyogenes**: *Streptococcus pyogenes*; **A. flavus**: *Aspergillus flavus*; **A. niger**: *Aspergillus niger*; **S. agalactiae**: *Streptococcus agalactiae*; **S. larcymans**: *Serpula larcymans*; **S. typhi**: *Salmonella typhi*; **S. epidermidis**: *Staphylococcus epidermidis*; **X. axonopodis**: *Xanthomonas axonopodis*; **P. acnes**: *Propionibacterium acnes*; **A. alternata**: *Alternaria alternata*; **E. coccus**: *Enterococcus*; **MRSA**: Methicillin-Resistant *Staphylococcus aureus*; **S. larcymans**: *Serpula larcymans*.

CONFLICT OF INTEREST

The authors declare that there is no conflict of interest.

AUTHOR CONTRIBUTIONS

GSB: Conceptualization, writing original draft, Review and editing, Visualization. **AJ**: Review and editing. **TJ**: editing. **RNJ**: Writing original draft, Review and editing.

REFERENCES

- Mossa JS, Tariq M, Mohsin A, Ageel AM, Al-Yahya MA, Al-Said MS, et al. Pharmacological studies on aerial parts of *Calotropis procera*. Am J Chin Med. 1991; 19(3-4): 223-31. doi: 10.1142/S0192415X91000302, PMID 1767794.
- Srikanth SK, Giri DD, Pal DB, Mishra PK, Upadhyay SN. Green synthesis of silver nanoparticles: a review. Green Sustain Chem. 2016; 6(1): 34-56. doi: 10.4236/gsc.2016.61004.
- Murti Y, Yogi B, Pathak D. Pharmacognostic standardization of leaves of *Calotropis procera* (Ait.) R. Br. (Asclepiadaceae). Int J Ayurveda Res. 2010; 1(1): 14-7. doi: 10.4103/0974-7788.59938, PMID 20532092.
- Hassan MH, Ismail MA, Moharram AM, Shoreit AA. Phytochemical and antimicrobial of latex serum of *Calotropis procera* and its silver nanoparticles against some reference pathogenic strains. J Ecol Health Environ. 2017; 5(3): 65-75. doi: 10.18576/jeh/050301.
- Ramadan A, Sabir JS, Alakilli SY, Shokry AM, Gadalla NO, Edris S, et al. Metabolomic response of *Calotropis procera* growing in the desert to changes in water availability. PLOS One. 2014; 9(2): e87895. doi: 10.1371/journal.pone.0087895, PMID 24520340.
- Yadi M, Mostafaei E, Saleh B, Davaran S, Aliyeva I, Khalilov R, et al. Current developments in green synthesis of metallic nanoparticles using plant extracts: a review. Artif Cells Nanomed Biotechnol. 2018; 46 sup3:5336-43. doi: 10.1080/21691401.2018.1492931, PMID 30043657.
- Li Y, Wu TY, Chen SM, Ali MA, AlHemaid FM. Green synthesis and electrochemical characterizations of gold nanoparticles using leaf extract of *Magnolia Kobus*. Int J Electrochem Sci. 2012; 7(12): 12742-51. doi: 10.1016/S1452-3981(23)16581-3.
- Varadavenkatesan T, Vinayagam R, Selvaraj R. Structural characterization of silver nanoparticles phyto-mediated by a plant waste, seed hull of *Vigna mungo*, and their biological applications. J Mol Struct. 2017; 1147: 629-35. doi: 10.1016/j.molstruc.2017.07.002.
- Habeeb A, Ramesh S, Shanmugam R. *Calotropis procera* and the pharmacological properties of its aqueous leaf extract: a review. Cureus. 2024; 16(5): e60354. doi: 10.7759/cureus.60354, PMID 38883127.
- Jain A, Jangid T, Jangir RN, Bhardwaj GS. A comprehensive review on the antioxidant properties of green synthesized nanoparticles: *in vitro* and *in vivo* insights. Free Radic Antioxid. 2025; 14(2): 34-61. doi: 10.5530/fra.2024.2.6.
- Al Sulaibi MA, Thiemann C, Thiemann T. Chemical constituents and uses of *Calotropis procera* and *Calotropis gigantea* – a review (Part I – the plants as material and energy resources). Open Chem J. 2020; 7(1): 1-15. doi: 10.2174/1874842202007010001.
- Parihar G, Balekar N. *Calotropis procera*: a phytochemical and pharmacological review. Thai J Pharm Sci. 2016; 40(3): 115-31. doi: 10.56808/3027-7922.1918.
- Verma R, Satsangi GP, Shrivastava JN. Ethno-medicinal profile of different plant parts of *Calotropis procera* (Ait.) R. Br Ethnobot Leaflet. 2010; 14: 721-42.
- Abhishek D, Chaturvedi M, Gupta A, Argal A. Medicinal utility of *Calotropis procera* (Ait.) R. Br. as used by natives of village Sanwer of Indore District, Madhya Pradesh. Int J Pharm Life Sci. 2010; 1(3): 188-90.

15. Al-Rowaily SL, Abd-ElGawad AM, Assaeed AM, Elgamal AM, Gendy AE, Mohamed TA, et al. Essential oil of *Calotropis procera*: comparative chemical profiles, antimicrobial activity, and allelopathic potential on weeds. *Molecules*. 2020; 25(21): 5203. doi: 10.3390/molecules25215203, PMID 33182287.
16. Aliyu RM, Abubakar MB, Kasarawa AB, Dabai YU, Lawal N, Bello MB, et al. Efficacy and phytochemical analysis of latex of *Calotropis procera* against selected dermatophytes. *J Intercult Ethnopharmacol*. 2015; 4(4): 314-7. doi: 10.5455/jice.20151012012909, PMID 26649237.
17. Ahmed KK, Rana AC, Dixit VK. *Calotropis* species (*Asclepiadaceae*): a comprehensive review. *Pharmacogn Mag*. 2005; 1(2): 48-52.
18. Mainasara MM, Aliero BL, Aliero AA, Dahiru SS. Phytochemical and antibacterial properties of *Calotropis procera* (Ait) R. Br. (Sodom apple) fruit and bark extracts. *Int J Mod Bot*. 2011; 1(1): 8-11. doi: 10.5923/jijmb.20110101.03.
19. Shrivastava A, Singh S, Singh S. Phytochemical investigation of different plant parts of *Calotropis procera*. *Int J Sci Res Publ*. 2013; 3(3): 1-4.
20. Saber H, Maharan GH, Rizkallah MM. Sterols and pentacyclic triterpenes of *Calotropis procera*. *Bol Fac Pharm*. 1969; 7: 91-104.
21. Deepak D. The taxonomy and phytochemistry of the Asclepiadaceae in tropical Asia. In: Botany Asia International Seminar and Workshop; 1994; Malacca, Selangor, Malaysia. Universiti Pertanian Malaysia; 2000. p. 1995.
22. Tiwari KP, Masood YK, Rathore S, Minocha PK. Study of anthocyanins from the flowers of some medicinal plants. *Vijnana Parishad Anusandhan Patrika*. 1978; 21: 177-8.
23. Ansari SH, Ali M. New oleanene triterpenes from root bark of *Calotropis procera*. *Indian J Chem*. 1999; 39: 287-90.
24. Carruthers IB, Griffiths DJ, Home V, Williams LR. Hydrocarbons from *Calotropis procera* in Northern Australia. *Biomass*. 1984; 4(4): 275-82. doi: 10.1016/0144-4565(84)90040-4.
25. Kakkar A, Verma DR, Suryavanshi S, Dubey P. Characterization of chemical constituents of *Calotropis procera*. *Chem Nat Compd*. 2012; 48(1): 155-7. doi: 10.1007/s10600-012-0189-1.
26. Mittal A, Ali M. Acyclic diterpenic constituents from the roots of *Calotropis procera* (Ait.) R. Br. *J Saudi Chem Soc*. 2015; 19(1): 59-63. doi: 10.1016/j.jssc.2011.12.019.
27. Rani R, Sharma D, Chaturvedi M, Yadav JP. Phytochemical analysis, antibacterial and antioxidant activity of *Calotropis procera* and *Calotropis gigantea*. *J Nat Prod*. 2019; 9(1): 47-60. doi: 10.2174/2210315508666180608081407.
28. Nenaah G. Antimicrobial activity of *Calotropis procera* Ait. (*Asclepiadaceae*) and isolation of four flavonoid glycosides as the active constituents. *World J Microbiol Biotechnol*. 2013; 29(7): 1255-62. doi: 10.1007/s11274-013-1288-2, PMID 23417281.
29. Shukla OP, Krishnamurthy CR. Properties and partial purification of bacteriolytic enzyme from the latex of *Calotropis procera* (Madar). *J Sci Ind Res*. 1961; 20: 109-12.
30. Chundattu SJ, Agrawal VK, Ganesh N. Phytochemical investigation of *Calotropis procera*. *Arab J Chem*. 2016; 9: S230-4. doi: 10.1016/j.arabjc.2011.03.011.
31. Mohamed NH, Liu M, Abdel-Mageed WM, Alwahibi LH, Dai H, Ismail MA, et al. Cytotoxic cardenolides from the latex of *Calotropis procera*. *Bioorg Med Chem Lett*. 2015; 25(20): 4615-20. doi: 10.1016/j.bmcl.2015.08.044, PMID 26323871.
32. Ali MS, Altaf M, Al-Lohedan HA. Green synthesis of biogenic silver nanoparticles using *Solanum tuberosum* extract and their interaction with human serum albumin: evidence of "corona" formation through a multi-spectroscopic and molecular docking analysis. *J Photochem Photobiol B*. 2017; 173: 108-19. doi: 10.1016/j.jphotobiol.2017.05.015, PMID 28570906.
33. Maisam M, Lodhi MS, Sharif S, Anees R, Anwar RI, Inam M, et al. Biofabricated silver nanoparticles from *Calotropis procera*: a potential antimicrobial solution against pathogenic bacteria. *Int J Appl Exp Biol*. 2022; 4(1): 27-39. doi: 10.56612/ijaaeb.v1i1.107.
34. Nagime PV, Shaikh NM, Shaikh SB, Lokhande CD, Patil VV, Shafi S, et al. Facile synthesis of silver nanoparticles using *Calotropis procera* leaves: unraveling biological and electrochemical potentials. *Discov Nano*. 2024; 19(1): 139. doi: 10.1186/s11671-024-04090-w, PMID 39227530.
35. Murshed M, Al-Tamimi J, Mares MM, Hailan WA, Ibrahim KE, Al-Quraishy S. Pharmacological effects of biosynthesis silver nanoparticles utilizing *Calotropis procera* leaf extracts on Plasmodium berghei-infected liver in experimental mice. *Int J Nanomedicine*. 2024; 19: 13717-33. doi: 10.2147/IJN.S490119, PMID 39726977.
36. Raj S, Muthu D, Isaac RS, Ramakrishnan S, S AE, Vallinayagam S. Nanomedicinal evaluation of *Calotropis procera*-mediated silver nanoparticle on skin cancer cell line for microbes-front line analysis. *J Mol Struct*. 2021; 1235: 130237. doi: 10.1016/j.molstruc.2021.130237.
37. Ghramh HA, Ibrahim EH, Ahmad Z. Antimicrobial, immunomodulatory and cytotoxic activities of green synthesized nanoparticles from Acacia honey and *Calotropis procera*. *Saudi J Biol Sci*. 2021; 28(6): 3367-73. doi: 10.1016/j.sjbs.2021.02.085, PMID 34121874.
38. Harisma BR, Annis CJ, Begum SB, Kalpana R, Murugappan R. Utilization of herbivore defensive latex from the weed *Calotropis procera* L. in the green synthesis of silver nanoparticles and its potential application in the control of dengue vector *Aedes aegypti*. *J Nat Pestic Res*. 2024; 9:100073: 1-6. doi: 10.1016/j.napere.2024.100073.
39. Jain PK, Lee KS, El-Sayed IH, El-Sayed MA. Calculated absorption and scattering properties of gold nanoparticles of different size, shape, and composition: applications in biological imaging and biomedicine. *J Phys Chem B*. 2006; 110(14): 7238-48. doi: 10.1021/jp057170o, PMID 16599493.
40. Sperling RA, Rivera Gil PR, Zhang F, Zanella M, Parak WJ. Biological applications of gold nanoparticles. *Chem Soc Rev*. 2008; 37(9): 1896-908. doi: 10.1039/b712170a, PMID 18762838.
41. Huang X, El-Sayed MA. Gold nanoparticles: optical properties and implementations in cancer diagnosis and photothermal therapy. *J Adv Res*. 2010; 1(1): 13-28. doi: 10.1016/j.jare.2010.02.002.
42. Jeong S, Choi SY, Park J, Seo JH, Park J, Cho K, et al. Low-toxicity chitosan gold nanoparticles for small hairpin RNA delivery in human lung adenocarcinoma cells. *J Mater Chem*. 2011; 21(36): 13853-9. doi: 10.1039/c1jm11913c.
43. Jadoun S, Arif R, Jangid NK, Meena RK. Green synthesis of nanoparticles using plant extracts: a review. *Environ Chem Lett*. 2021; 19(1): 355-74. doi: 10.1007/s10311-020-01074-x.
44. Shittu OK, Stephen DI. Cytotoxicity property of biologically synthesized gold nanoparticles from aqueous leaf extract of *Calotropis procera* (Apple of Sodom) on MCF-7 cell line. *Br J Med Med Res*. 2016; 15(12): 1-8. doi: 10.9734/BJMMR/2016/26385.
45. Oladipo CI. Phytosynthesis of gold nanoparticles from *Calotropis procera* leaf aqueous extract: antihypertensive, antioxidant and antifungal activities. *Adv Earth Environ Sci*. 2024; 5(4): 1-7.
46. Adams FC, Barbante C. Nanoscience, nanotechnology and spectrometry. *Spectrochim Acta B*. 2013; 86: 3-13. doi: 10.1016/j.sab.2013.04.008.
47. Ahmed S, Annu SA, Chaudhry SA, Ikram S. A review on biogenic synthesis of ZnO nanoparticles using plant extracts and microbes: a prospect towards green chemistry. *J Photochem Photobiol B*. 2017; 166: 272-84. doi: 10.1016/j.jphotobiol.2016.12.011, PMID 28013182.
48. Agarwal H, Kumar SV, Rajeshkumar S. A review on green synthesis of zinc oxide nanoparticles – an eco-friendly approach. *Resour Eff Technol*. 2017; 3: 406-13.
49. Sharma R, Sharma H, Pareek A, Lodha P. Eco-friendly synthesis of ZnO nanoparticles from *Calotropis procera* and their *in vivo* nematocidal potential. *SSR-IJLS*. 2025; 11(2): 7178-85. doi: 10.21276/SSR-IJLS.2025.11.2.27.
50. El-Fitany RA, AlBlooshi A, Samadi A, Khasawneh MA. Biogenic synthesis and physicochemical characterization of metal nanoparticles based on *Calotropis procera* as promising sustainable materials against skin cancer. *Sci Rep*. 2024; 14(1): 25154. doi: 10.1038/s41598-024-76422-w, PMID 39448765.
51. Srilatha D, Arunasri K, Sravanthi M. Synthesis, characterization and antimicrobial activity of zinc oxide nanoparticles synthesized from *Calotropis procera*. *Int J Life Sci Biotechnol PharmSci*. 2024; 20(1): 6-14.
52. Reddy KR. Green synthesis, morphological and optical studies of CuO nanoparticles. *J Mol Struct*. 2017; 1150: 553-7. doi: 10.1016/j.molstruc.2017.09.005.
53. Li J, Sun F, Gu K, Wu T, Zhai W, Li W, et al. Preparation of spindle CuO micro-particles for photodegradation of dye pollutants under a halogen tungsten lamp. *Appl Catal A*. 2011; 406(1-2): 51-8. doi: 10.1016/j.apcata.2011.08.007.
54. Dubey S, Sharma C. C. *procera*-mediated one-pot green synthesis of cupric oxide nanoparticles for adsorptive removal of Cr(IV) from aqueous solution. *Appl Organomet Chem*. 2017; 31(12): 39-41.
55. Sethupandian DM, Sugi DL, Sakthivel DP, Ambigai MK. Green synthesized CuO nanoparticles with seed extract of *Calotropis procera* and their antibacterial activity. *SSRN*. 2023; 1-9. doi: 10.2139/ssrn.4354186.
56. Huang Z, Cui F, Kang H, Chen J, Zhang X, Xia C. Highly dispersed silica-supported copper nanoparticles prepared by precipitation-gel method: a simple but efficient and stable catalyst for glycerol hydrogenolysis. *Chem Mater*. 2008; 20(15): 5090-9. doi: 10.1021/cm8006233.
57. Harne S, Sharma A, Dhaygude M, Joglekar S, Kodam K, Hudlikar M. Novel route for rapid biosynthesis of copper nanoparticles using aqueous extract of *Calotropis procera* L. latex and their cytotoxicity on tumor cells. *Colloids Surf B Biointerfaces*. 2012; 95: 284-8. doi: 10.1016/j.colsurfb.2012.03.005, PMID 22483347.
58. Arumugam A, Karthikeyan C, Haja Hameed AS, Gopinath K, Gowri S, Karthika V. Synthesis of cerium oxide nanoparticles using *Gloriosa superba* L. leaf extract and their structural, optical and antibacterial properties. *Mater Sci Eng C Mater Biol Appl*. 2015; 49: 408-15. doi: 10.1016/j.msec.2015.01.042, PMID 25686966.
59. Muthuvel A, Jothibas M, Mohana V, Manoharan C. Green synthesis of cerium oxide nanoparticles using *Calotropis procera* flower extract and their photocatalytic degradation and antibacterial activity. *Inorg Chem Commun*. 2020; 119: 108086. doi: 10.1016/j.inoche.2020.108086.
60. Ali M, Haroon U, Khizar M, Chaudhary HJ, Munis MF. Facile single-step preparations of phyto-nanoparticles of iron in *Calotropis procera* leaf extract to evaluate their antifungal potential against *Alternaria alternata*. *Curr Plant Biol*. 2020; 23: 100157. doi: 10.1016/j.cpb.2020.100157.
61. Hsu CY, Mahmood ZH, Abdullaev S, Ali FK, Naeem YA, Mizher RM, et al. Nano titanium oxide (nano-TiO₂): a review of synthesis methods, properties, and applications. *Case Stud Chem Environ Eng*. 2024; 9: 100626.
62. Suhag R, Kumar R, Dhiman A, Sharma A, Prabhakar PK, Gopalakrishnan K, et al. Fruit peel bioactives, valorisation into nanoparticles and potential applications: a review. *Crit Rev Food Sci Nutr*. 2023; 63(24): 6757-76. doi: 10.1080/10408398.2022.2043237, PMID 35196934.
63. Vieira IR, de Carvalho AP, Conte-Junior CA. Recent advances in bio-based and biodegradable polymer nanocomposites, nanoparticles, and natural antioxidants for antibacterial and antioxidant food packaging applications. *Compr Rev Food Sci Food Saf*. 2022; 21(4): 3673-716. doi: 10.1111/1541-4337.12990, PMID 35713102.

64. Fatima M, Anjum T, Manzoor M, Aftab M, Aftab ZE, Akram W, et al. Green synthesis and characterization of TiO₂ nanoparticles from latex of *Calotropis procera* against dusky cotton bug. *Sci Rep*. 2025; 15(1): 11102. doi: 10.1038/s41598-024-82841-6, PMID 40169618.
65. Hidayat MF, Mufti N, Latifah E. Study on distribution of magnetite (Fe_{3-x}Mn_xO₄) filler in Fe_{3-x}Mn_xO₄-PEG/PVA/PVP magnetic hydrogel by using two lognormal function analysis. *IOP Conf Ser Mater Sci Eng*. 2019; 515: 012024. doi: 10.1088/1757-899X/515/1/012024.
66. Kalu AO, Egwim EC, Jigam AA, Muhammad HL. Green synthesis of magnetite nanoparticles using *Calotropis procera* leaf extract and evaluation of its antimicrobial activity. *Nano Express*. 2022; 3(4): e015027. doi: 10.1088/2632-959X/aca925.
67. Aina DA, Animashaun OH. *Calotropis procera*-mediated synthesis of silver nanoparticles and its antibacterial effect on selected pathogens. *Asian Plant Res J*. 2024; 12(6): 69-77. doi: 10.9734/aprj/2024/v12i6282.
68. Jahan N, Fahmid S, Jabeen U, Hayat A, Zahid S, Bashir F, et al. Synthesis of gold nanoparticles from *Calotropis procera* and *Colutea armata*: assessment of antifungal activity against *Serpula lacrymans*. *Pure Appl Biol*. 2023; 13(1): 55-68. doi: 10.19045/bspab.2024.130006.
69. Mamman AJ, Myek B, Ladan Z. Green synthesized silver nanoparticles (AgNPs) using aqueous extract of *Calotropis procera* and its antimicrobial activity on clinical bacteria isolates. *Sci World J*. 2023; 18(4): 662-9. doi: 10.4314/swj.v18i4.19.
70. Nazeer WW, Hassanein EM, Barakat NA. Green synthesis of silver nanoparticles using *Calotropis procera* and *Amaranthus ascendens* stem extracts and evaluation of their antimicrobial activity. *Afr J Biol Sci*. 2023; 19(1): 53-67.
71. Mohideen MA, Mumtaz M, Iyyadurai M, Rajan GR, Kumar DJ. *Calotropis procera* leaf extract-based zinc oxide nanoparticles synthesis and antimicrobial study. *Soc Evol Hist*. 2025; 14(1): 95-106.
72. Vivek V, Sethi N, Kaura S. Green synthesis and evaluation of antibacterial activity of zinc nanoparticles from *Calotropis procera* leaves. *J Pharm Innov J*. 2022; 11(10): 1551-4.
73. Chandru M, Logesh R, Kutti Rani S, Ahmed N, Vasimalai N. Green synthesis of silver nanoparticles from plant latex and their antibacterial and photocatalytic studies. *Environ Technol*. 2022; 43(20): 3064-74. doi: 10.1080/09593330.2021.1914181, PMID 33825663.
74. Salmen SH, Alkammash NM, Alahmadi TA, Alharbi SA. Characterization and antibacterial activity of silver nanoparticles biosynthesized using leaves extract of *Artemisia sieberi* and *Calotropis procera*. *Rev Chim*. 2021; 72(2): 76-82. doi: 10.37358/RC.21.2.8421.
75. Sagadevan S, Vennila S, Muthukrishnan L, Gurunathan K, Oh WC, Paiman S, et al. Exploring the therapeutic potentials of phyto-mediated silver nanoparticles formed via *Calotropis procera* (Ait.) R. Br. root extract. *J Exp Nanosci*. 2020; 15(1): 217-31. doi: 10.1080/17458080.2020.1769842.
76. Poovizhi J, Krishnaveni B. Synthesis, characterization and antimicrobial activity of zinc oxide nanoparticles synthesized from *Calotropis procera*. *Int J Pharm Sci Drug Res*. 2015; 7(5): 425-31.
77. Mohamed NH, Ismail MA, Abdel-Mageed WM, Mohamed Shoreit AA. Antimicrobial activity of latex silver nanoparticles using *Calotropis procera*. *Asian Pac J Trop Biomed*. 2014; 4(11): 876-83. doi: 10.12980/APJTB.4.201414B216.
78. Adeyemo AG, Igbalaye OJ, Awote OK, Apete SK, Kanmodi RI, Saibu GM, et al. Characterization and antioxidant potential of silver nanoparticles (AgNPs) synthesized using the aqueous leaf extract of *Calotropis procera*: an *in vitro* study. *South Asian Res J Nat Prod*. 2022; 5(3): 1-10.
79. Thasleem AE, Umesh BT, Joseph V. Phytochemical investigations and green synthesis of nanoparticles from *Calotropis procera*. *Int J Novel Res Dev*. 2023; 8(9). ISSN: 2456-4184.
80. Masood L, Ahmad S, Iqbal M, Chattha AJ, Ashraf S, Hussain T, et al. Insecticidal activity of green synthesized zinc oxide nanoparticles from *Calotropis procera* against fall armyworm. *Int J Biol Biotechnol*. 2024; 21(4): 483-91.
81. Devi MC, Jameela MS, Asharaja A, Rajan GR, Iyyadurai M, Reegan AD. Effect of *Calotropis procera* (Aiton) Dryand. based zinc oxide nanoparticles on the cotton pest *Spodoptera litura* Fab. *Indian J Exp Biol*. 2023; 61(3): 224-9. doi: 10.56042/ijeb.v61i03.68093.
82. Pushparani DS, Iniya M, Srinivasan PT. Insecticidal effects of biosynthesized silver nanoparticles from *Calotropis* species on *Tribolium castaneum*. *Int J Pharm Sci Rev Res*. 2023; 79(1): 69-74. doi: 10.47583/ijpsrr.2023.v79i01.014.
83. Basak SK, Bhaumik A, Mohanta A, Singhal P. Ocular toxicity by latex of *Calotropis procera* (Sodom apple). *Indian J Ophthalmol*. 2009; 57(3): 232-4. doi: 10.4103/0301-4738.49402, PMID 19384022.
84. Dogara AM. A systematic review on the biological evaluation of *Calotropis procera* (Aiton) Dryand. *Future J Pharm Sci*. 2023; 9(1): 1-19. doi: 10.1186/s43094-023-00467-3.
85. Kumari I, Chaudhary G. *Calotropis procera* (Arka): a tribal herb of utmost significance. *Int J Res Appl Sci Biotechnol*. 2021; 8(3): 44-54. doi: 10.31033/ijrasb.8.3.8.
86. Devasari T. Toxic effects of *Calotropis procera*. *Indian J Pharmacol*. 1965; 27: 272-5.
87. Al-Zuhairi AH, Khalaf Al-Ani JM, Ibrahim SN. Toxicological effects of aqueous extract of *Calotropis procera* leaves in experimentally poisoned rabbits. *Iraqi J Vet Med*. 2020; 44(1): 46-56. doi: 10.30539/ijvm.v44i1.934.
88. Habib S, Rashid F, Tahir H, Liaqat I, Latif AA, Naseem S, et al. Antibacterial and cytotoxic effects of biosynthesized zinc oxide and titanium dioxide nanoparticles. *Microorganisms*. 2023; 11(6): 1363. doi: 10.3390/microorganisms11061363, PMID 37374866.

Cite this article: Bhardwaj GS, Jain A, Jangid T, Jangir RN. A Comprehensive Review of the Pharmacological Potential of Green Synthesized Nanoparticles from *Calotropis procera*. *Pharmacog Rev*. 2025;19(38):236-59.